Quaternary Science Reviews 344 (2024) 108977

Contents lists available at ScienceDirect

Quaternary Science Reviews

journal homepage: www.elsevier.com/locate/quascirev

Late-Holocene ecosystem dynamics on Weizhou Island, China: A pollen and historical record of climate change and anthropogenic disturbances

Yuanfu Yue [a], Xi Xiang [a], Dan Zhao [b], Shixiong Yang [c,d,**], Qiang Yao [e,*]

[a] School of Marine Sciences, Coral Reef Research Center of China, Guangxi University, Guangxi Laboratory on the Study of Coral Reefs in the South China Sea, Nanning 530004, China
[b] College of Landscape Architecture, Sichuan Agriculture University, Chengdu, China
[c] Key Laboratory of Coastal Wetland Biogeosciences, Qingdao Institute of Marine Geology, China Geological Survey, 266071 Qingdao, China
[d] Laboratory for Marine Geology, Qingdao Marine Science and Technology Center, 266237 Qingdao, China
[e] Department of Oceanography and Coastal Sciences, College of the Coast and Environment, Louisiana State University, Baton Rouge, LA, United States

ARTICLE INFO

Handling editor: Yan Zhao

Keywords:
Palynology
Historical documents
Charcoal particles
Weizhou island
Vegetation succession
Biodiversity
Environmental change
Anthropogenic disturbances

ABSTRACT

Understanding the mechanisms behind landscape diversity changes on islands, particularly due to historical human interventions, remains a critical challenge in paleoecology. This study addresses this gap by utilizing over 160 pollen samples combined with multi-proxy data and historical records to reconstruct the late-Holocene ecological and environmental dynamics of Weizhou Island, China, over the last 1400 years. Our analyses reveal the evolution of ecosystem diversity and vegetation succession amid climatic fluctuations and anthropogenic pressures, identifying four distinct phases of transformation: (1) A warm and dry climate from 1400 to 850 cal yr BP fostering a savanna ecosystem; (2) A shift to a North subtropical seasonal rainforest under a more humid climate between 850 and 210 cal yr BP, with increased vegetation diversity; (3) The initiation of agriculture and aquaculture, along with a cooler climate from 210 cal yr BP to 1970 CE, marked by human-induced landscape alterations; and (4) A significant transformation from a once-diverse ecosystem to artificial protective forests from 1970 CE to the present. By correlating environmental indicators with historical accounts across eight Chinese dynasties, our study provides detailed insights into the climatic and human factors shaping the island's history. The findings demonstrate that while climatic shifts are primary drivers of biodiversity changes, anthropogenic disturbances also play a significant role. This research underscores the resilience of ecosystems to both climatic and human pressures and emphasizes the importance of integrating historical context into environmental studies.

1. Introduction

In coastal environments, vegetation succession and ecosystem dynamics are profoundly influenced by natural forces such as tidal fluctuations (Kim et al., 2011; Bakker et al., 2016), extreme disturbance events (e.g., flooding, wildfires, and tropical storms) (Yue et al., 2019; Yu et al., 2021; 2023a), sea level rise (FitzGerald and Hughes, 2019; Nienhuis et al., 2023), and climatic factors like temperature (Rodrigues et al., 2021), solar insolation (Corenblit and Steiger, 2009), and precipitation regimes (De Steven and Toner, 2004; Zhang et al., 2021a). These elements, coupled with other biotic and abiotic factors and climatic variations, collectively shape the unique and dynamic nature of coastal ecosystems, modulating plant species richness and ecological progression (Prach and Walker, 2011; Chang and Turner, 2019; Yao and Liu, 2017, 2022a).

However, over the past millennium, global ecosystems are increasingly shaped by the accelerating climate change (Harley et al., 2006; Waycott et al., 2009; Doney et al., 2012). As a result, there has been a marked transition from ecosystem dynamics being predominantly driven by natural forces to a state where anthropogenic activities significantly contribute to environmental changes (Yue et al., 2024a; Zheng et al., 2021), especially coastal environments across the globe

* Corresponding author. Department of Oceanography and Coastal Sciences, College of the Coast and Environment, Louisiana State University, Baton Rouge, LA, United States.
** Corresponding author. Key Laboratory of Coastal Wetland Biogeosciences, Qingdao Institute of Marine Geology, China Geological Survey, 266071 Qingdao, China.
E-mail addresses: yshixiong@mail.cgs.gov.cn (S. Yang), qyao4@lsu.edu (Q. Yao).

https://doi.org/10.1016/j.quascirev.2024.108977
Received 27 March 2024; Received in revised form 21 August 2024; Accepted 16 September 2024
Available online 19 September 2024

(Jackson et al., 2001; He and Silliman, 2019). This shift has made it imperative to understand the cumulative impacts of these influences on ecosystem dynamics and biodiversity. The rapid pace of environmental change, driven by factors such as warming, deforestation, urbanization, and pollution, underscores the urgency for comprehensive, long-term datasets. These datasets are essential to decipher the complex relationships between natural processes and human activities, and their cumulative effects on vegetation succession (Ge and Zhu, 2021; Wang et al., 2021).

In this context, natural and undisturbed islands, as quintessential examples of coastal ecosystems, are increasingly confronted with resource depletion and ecological vulnerability due to their distinctive geographical positions (Russell and Kueffer, 2019; Yao et al., 2023b). Their location at the nexus of land and sea renders them vital for understanding ecological responses to long-term and extreme natural disturbances (Barbier, 2015; Nwipie et al., 2019). Their relatively pristine state provides a clearer picture of the inherent ecological processes and baseline conditions, allowing scientists to distinguish between natural ecological dynamics and changes driven by human interference (Liu et al., 2021). Research focused on the vegetation succession of these islands can yield valuable insights into how these ecosystems adapt to and are reshaped by environmental stressors. This knowledge is crucial for predicting the future of these fragile ecosystems amidst ongoing global changes and for informing conservation efforts (Kirwan and Megonigal, 2013). However, long-term records of ecological succession and species richness from pristine tropical and subtropical islands are remarkably rare (Colinvaux and Schofield, 1976; Wilmshurst et al., 2014). Thus, a large gap exists in the paleoecological data network.

Weizhou Island (20°54′-21°10′N. 109°00′-109°15′E; Fig. 1), a small island situated at the center of Beibu Gulf, exemplifies its critical location at the forefront of the land-sea transition in the South China Sea. With a small size of ~25 km^2, Weizhou Island is particularly sensitive to climatic fluctuations and natural disturbances such as sea level rise, floods, and tropical cyclones (Yue et al., 2019, 2024b; Zhu et al., 2012). Its well-developed wetlands and substantial depositional history have the potential to record extensive baseline data on climate variations in South Asia's subtropical region (Wang et al., 1991; Liao et al., 2012). This island lies in the northern South China Sea, adjacent to the tropical Western Pacific's warm pool, making it an ideal location to study the genesis and pattern of typhoon landfall. Additionally, it is among the

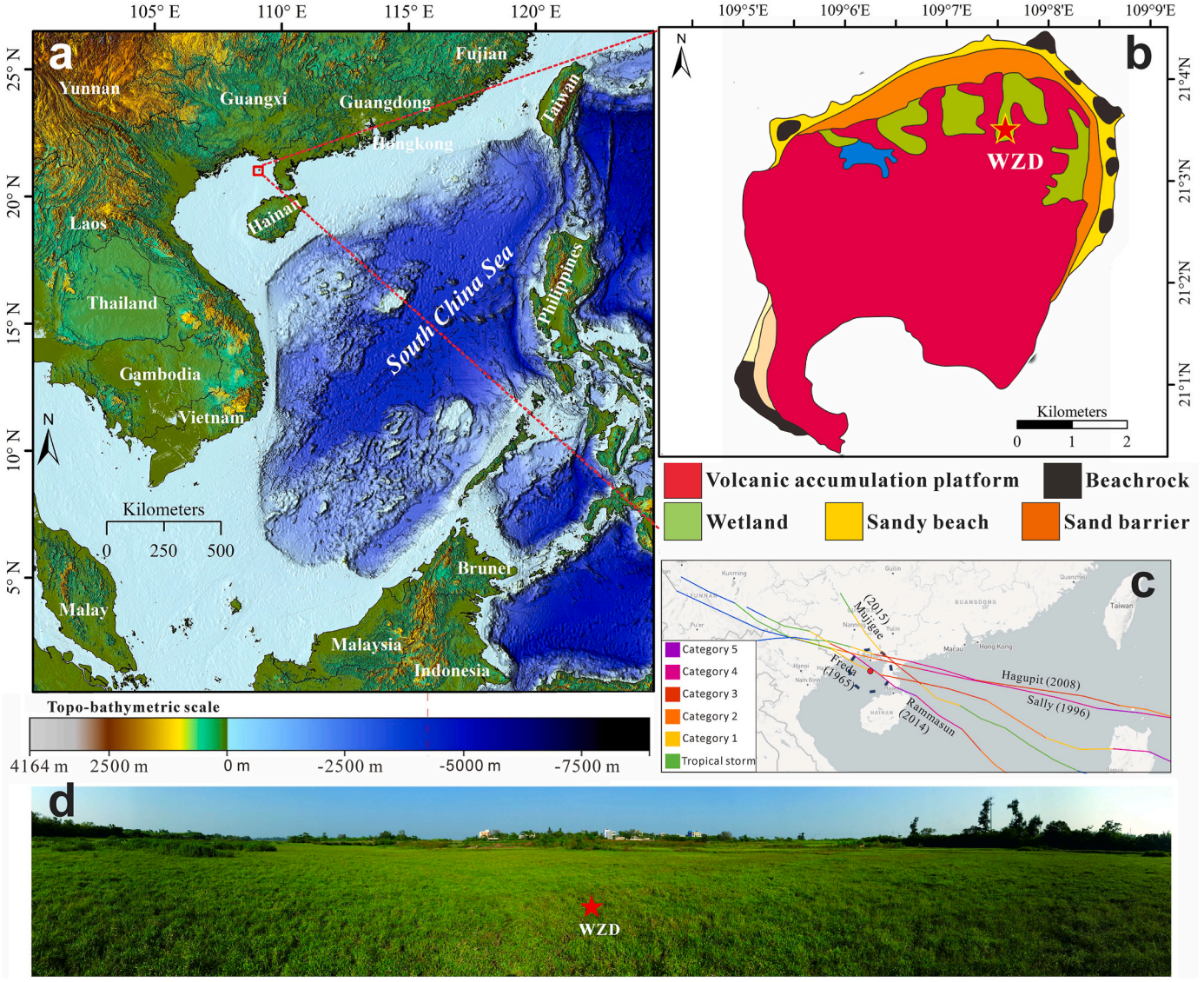

Fig. 1. Maps of the study area: (a) Digital Topo-bathymetric Model of the South China Sea; (b) Terrain map of Weizhou Island (modified from Qi et al. (2003)); (c) Storm tracks of the catastrophic typhoons passing Weizhou Island (National Oceanic and Atmospheric Administration, 2024). The circle masks the 100 km radius from the center of the island; (d) Photographs of the study area on Weizhou Island. Red star marks our coring site for WZD.

most dynamic zones for air-sea interaction (Liang and Wan, 1995; Liao et al., 2012). The shielding effect of Hainan Island attenuates the impact from South China Sea currents on Weizhou Island, positioning it as an optimal location for paleoecological research (Zhang et al., 2020).

Prior research on the Holocene environmental evolution of Weizhou Island has been somewhat disconnected from the broader environmental history of subtropical South Asia, largely due to the lack of accurate radiocarbon dating. This gap has led to a fragmented understanding of environmental changes over the past millennium. In this study, we present a well-dated core WZD (160 cm), containing lacustrine-swamp facies deposits spanning the last ~1400 years from the northeast side of the island, and utilize palynology, microcharcoal and grain-size analyses, and historical document to reconstruct the paleoclimatic and environmental history of the Beibu Gulf region since the late-Holocene. The overarching objective of this study is to decipher the history of human-environment interactions and the consequential regional vegetation succession, and to understand the roles of climate change, historical human activity, and extreme disturbance events on the landscape dynamics, species richness, and ecosystem evolution of Weizhou Island.

2. Study area DESCRIPTION

2.1. Geomorphic background of Weizhou Island

Weizhou Island is the youngest and largest volcanic island in the northern part of the South China Sea (Fig. 1a). It is located ~39 km to the south of Beihai City and ~17 km southeast of Xieyang Island. Geographically positioned to the south of Hainan Province and to the west of Vietnam, Weizhou Island displays a distinct topographical gradient. The island's terrain exhibits a gradual southern-to-northern slope, culminating in an elliptical configuration, prominently featuring a crescent-shaped bay at the south side (Zhu et al., 2012). Spanning a length of 6.5 km from its northernmost to southernmost points and a breadth of 6 km from east to west, the island encompasses an area of ~25 km^2. The topographical variation is marked by a maximum elevation of 79 m, with the southern region presenting higher elevations that taper off towards the northern end, where elevations range between 20 and 40 m (Qi et al., 2003).

Geologically, Weizhou Island owes its origin to subaqueous eruptions of Quaternary basaltic magma. Over time, this volcanic activity, coupled with ongoing geological processes and evolutionary dynamics, has given rise to a diverse array of geomorphological features on the island (Qi et al., 2003). These include, but are not limited to, volcanic accumulation terraces, wetland, sandbanks, beaches, and beach rocks, as depicted in Fig. 1b. This diverse terrain not only underscores the island's volcanic origins but also highlights its complex geological history.

2.2. Climate and meteorological background

Located at lower latitudes between 20°54′ and 21°10′N, Weizhou Island is characterized by a South Asian tropical maritime monsoon climate. This climatic zone is marked by pronounced monsoonal patterns, exhibiting northerly winds during the winter months and southerly winds throughout the summer. The island experiences well-defined dry (November–April) and wet (May–October) seasons, contributing to its overall mild climate. Additionally, Weizhou Island benefits from considerable solar exposure, averaging 2234 h of sunshine annually. Recent meteorological data indicates an average yearly rainfall of approximately 1450 mm, though this figure is subject to notable variations (Liao et al., 2012). This climatic profile plays a significant role in shaping the island's environmental conditions and ecological dynamics.

According to the instrumental data provided by the National Oceanic and Atmospheric Administration (2024), Weizhou Island has experienced landfalls from a total of 24 typhoons within a 100 km radius. Among these, five were classified as catastrophic (Fig. 1c), falling within Categories 3 to 5 on the Saffire-Simpson Scale. These include Typhoon Freda (1965), Sally (1996), Hagupit (2008), Rammasun (2014), and Mujigae (2015). These typhoons represent the most severe storms to affect the study area since the mid-20th century. Their occurrence indicates an average return period of approximately 34 years for major typhoon landfalls in the region (National Oceanic and Atmospheric, 2024). The meteorological characteristics of all typhoons making landfall within 100 km of Weizhou Island since 1950 are comprehensively detailed in the Supplementary Content Table S1. This data is crucial for understanding the frequency and impact of severe weather events in the region, informing both current and future mitigation and preparedness strategies.

2.3. Environmental and vegetation background

Recently, it is reported that the relative sea level in the northern South China Sea was ~1.5–2.3 m and ~1 m higher than the present level during the mid-Holocene and the period between 1780 and 840 cal yr BP, respectively (Yue et al., 2024b; Yue and Tang, 2023; Liu et al., 2020). The current rate of sea level rise in the northern South China Sea over the past 40 years has reached ~3.55 mm/yr (Yue and Tang, 2023). Field surveys conducted on Weizhou Island between 2015 and 2019 revealed the presence of extensive wetlands, likely formed from the sedimentary deposits of the ancient lagoon during the Holocene high sea level stand (Qi et al., 2003). These wetlands, not significantly influenced by fluvial deposits and primarily dependent on precipitation, contain sediments predominantly sourced from storm surges, windblown sand, dust, and weathering products from nearby elevated areas. This stable sedimentary composition establishes these wetlands as invaluable archives for studying the geological and ecological evolution of Weizhou Island. As illustrated in Fig. 1c, these wetlands are primarily located in Gongju Village in the northeast side of the island, and are characterized by elongated or patchy formations, covering a total area of approximately 2 km^2.

Historically, the vegetation on Weizhou Island was shaped by the South Asian tropical monsoon climate and displayed a rich diversity. However, field investigations have found no natural forests currently on the island. Instead, the secondary natural vegetation includes species such as *Melia azedarach*, *Morus alba*, *Ficus virens*, *Cinnamomum camphora*, *Casuarina equisetifolia*, *Acacia confusa*, *Leucaena leucocephala*, and *Eucalyptus robusta*. The island also hosts a significant presence of the fleshy, spiny cactus *Opuntia dillenii*. Cultivated vegetation comprises both economic crops and shade trees, including *Litchi chinensis*, *Dimocarpus longan*, *Artocarpus heterophyllus*, *Citrus maxima*, *Citrus reticulata*, *Durio zibethinus*, *Areca catechu*, *Saccharum officinarum*, *Musa nana*, *Arachis hypogaea*, *Zea mays*, *Ipomoea batatas*, *Oryza sativa*, and *Ficus concinna*. The vegetation distribution is relatively simple, with sandy beaches predominantly supporting *Sporobolus virginicus*, *Ipomoea pescaprae*, and *cactus communities*, transitioning inland to semi-evergreen shrubs, *Acacia confusa*, *Casuarina equisetifolia*, and artificial cactus forests (Liao et al., 2012).

3. Methods and materials

3.1. Field work

In May 2019, a 160 cm sediment core WZD (21°03′26″N, 109°07′26″E) were recovered from the wetlands at the northeast side of Weizhou Island (Fig. 1b), using a Russian peat-borer (5.5 cm diameter). We selected the coring site in the wetland area due to its high sediment accumulation rates and excellent preservation of organic material, including pollen and charcoal, essential for paleoecological studies. This location minimizes disturbance from hydrological events and provides a continuous, well-preserved sedimentary record. Pollen data from this site can offer regional signals over distances typically up to 50 km (Jacobson and Bradshaw, 1981), making it sufficient to infer broader environmental changes. Preliminary surveys indicated well-preserved

sediments with clear stratification, confirming the site's suitability. Before the core extraction, surface layer and debris were removed, followed by pushing the core into the sediment profile until refusal to capture the most complete depositional history possible. The core consists of four 50 cm segments. Upon the acquisition of the core samples, they were photographed, documented, and then sealed in PVC tubes with saran wrap. Additionally, each core segment is distinctly marked for identification. In the laboratory, the core segments were further subdivided for various analyses, guided by the sediment deposition rates and sediment types. All cores are currently stored in a cold room (4 °C) at the sample repository, School of Marine Sciences, Guangxi University.

3.2. Chronology

The chronology of core WZD was derived through radiocarbon and Short-lived isotope (^{210}Pb and ^{137}Cs) dating techniques. The activities of ^{210}Pb were measured at 2-cm intervals from a depth of 0–50 cm using a low-energy germanium gamma spectrometer in Nanjing Institute of Geography & Limnology Chinese Academy of Sciences. The sediment samples were dried for 48 h, homogenized with a mortar and pestle, packed into 60 mm test tubes, and sealed with epoxy for 10 days to prevent ^{222}Rn loss and to reach secular equilibrium for ^{210}Pb. Activities were calculated following the methods detailed in Maiti et al. (2010). A linear regression of the natural logarithm of excess ^{210}Pb (^{210}Pbex) was applied to examine the sediment accretion rate (Maiti et al., 2010). Seven samples, each comprising bulk organic sediment, were dispatched to Beta Analytic Inc., located in Miami, for Accelerator Mass Spectrometry (AMS) radiocarbon dating (Table 1). The term 'bulk organic sediment' in this context refers to plant debris that has undergone a meticulous pretreatment process. This process involves the exclusion of roots, shells, and other extraneous materials, employing an advanced pretreatment method. A comprehensive, step-by-step elucidation of this pretreatment protocol has been documented in a publication by Yao et al. (2022b) in the journal MethodsX and is also included as supplementary material for reference. The short-lived isotope and radiocarbon dating results were subsequently integrated into software R, package *Bacon*, for the construction of an age-depth model (Blaauw and Christen, 2011). In this study, all dates were transformed into calibrated years before present (cal yr BP), with the calibration rounded to the nearest decade. This calibration uses the standard chronological marker of 1950 CE as the zero point for calibrated years before present (0 cal yr BP).

3.3. Proxy analysis

One hundred and sixty samples were taken from core WZD at a 1-cm interval to determine the percentages and concentrations of pollen and charcoal particles (>10 mm in size), by using a Nikon microscope at 400 and 1000 magnifications. Over 500 grains of pollen and spores were identified for most of the sample to derive a statistical meaningful result. In the quantification of charcoal particles, they are categorized based on the length of their longest axis (D) into two groups: those with $D < 100$ μm and those with $D \geq 100$ μm. One tablet containing ~27,637 of Lycopodium spores was added to every sample as an exotic marker to aid the calculation of pollen concentration (grains/cm^3), following the formular:

$$\text{Pollen concentration} = P_c * L_a / L_c * V$$

where P_c is the number of fossil pollen counted, L_a is the number of *Lycopodium* spores added (27,637), L_c is the number of *Lycopodium* spores counted, and V is the volume of the sample. Published pollen keys by Tang et al. (2016), Wang et al. (1995), and others (Palynology Group of Paleobotany Research Office, 1976, 1982) were used as references for pollen identification. A step-by-step elucidation of the pollen preparation protocol has been documented in a publication by Yao et al. (2023c) in the journal MethodsX and is also included as supplementary material for reference.

Grain-size analysis was performed at a 1-cm interval through the core using a Malvern Mastersizer 3000 particle size analyzer (3500–0.01 μm), with a resolution of 0.01ϕ and <3% of relative error of repeated measurements, at Guangxi Laboratory on the Study of Coral Reef in the South China Sea (Guangxi Universtiy). To ensure the accuracy of the measurement results, each sample was measured three times. Samples with significant errors in the measurement results were re-measured. The distribution of sand (2000–62.5 μm), silt (62.5–3.9 μm), and clay fraction (3.9–0.12 μm) was determined following the protocol developed by Wentworth (1922).

3.4. Rarefaction analysis

Palynological richness analysis was applied to core WZD using the rarefaction analysis with software PAST (PALEONTOLOGICAL STATISTICS SOFTWARE PACKAGE) (Hammer and Harper, 2001). Rarefaction analysis is a statistical method used to standardize samples of different pollen count, allowing for a more accurate estimate of average palynological richness with a constant pollen count, which is usually the sample with the lowest pollen count in all pollen samples (Birks and Line, 1992). An estimate of E (S_n) is given by:

$$E(S_n) = \sum_{i=1}^{s} \left(1 - \left[\frac{(N - N_i)!(N - N_{com})!}{(N - N_i - N_{com})!N!}\right]\right)$$

Where E (S_n) is the estimated number of pollen types in a sample of n selected at random without replacement from a count of N grains containing S taxa, S is the number of detected pollen types in the original count, N is the total number of pollen count of each sample, N_i is the number of original detected pollen grains of pollen taxon i, N_{com} is the new constant number of pollen count for all samples.

In this study, we are using the E (S_n) obtained by rarefaction analysis without any corrections, as a measure of species richness, vegetation composition, and landscape diversity. Pollen assemblages in core WZD have high pollen sums and were counted at a 1 cm to achieve the highest resolution possible. Weizhou Island is a small island with a total of ~25 km^2, and the shielding effect of Hainan Island attenuates the impact from South China Sea currents. Thus, we believe rarefaction analysis yielded species richness at a landscape scale across Weizhou Island rather than at local scale. The palynological reconstruction can detect the impacts of environmental variations, climate change, and human influence on vegetation composition in terms of landscape diversity.

Table 1
Radiocarbon dating results for core WZD.

Lab ID	Depth (cm)	Material	^{13}C/^{12}C ratio (‰)	Conventional age (^{14}C yr BP)	Median (2σ, 95.4%, cal yr BP)	Min	Max
WZ-50	50	Organic sediment	−26.3	106.95 ± 0.40 pMC	Modern	N/A	N/A
WZ-80	80	Organic sediment	−23.2	400 ± 30	450	240	500
WZ-100	100	Organic sediment	−24.8	480 ± 30	540	420	630
WZ-120	120	Organic sediment	−25.7	840 ± 30	710	600	870
WZ-140	140	Organic sediment	−21.2	1220 ± 30	1040	860	1240
WZ-160	160	Organic sediment	−23.9	2050 ± 30	1800	N/A	N/A
WZ-160	160	Organic sediment	−24.9	1580 ± 30	1400	1220	1580

4. Results

4.1. Sediment stratigraphy

Following the classification standard by Yue et al. (2015), this study categorizes grain size fractions into three types: clay (<2 μm), silt (2–63 μm), and sand (>63 μm). Visual inspection and grain size results revealed that core WZD consists of five different types of sediment (Fig. 2), including fine sand at the top (0–5 cm), brownish silt (5–25 cm) rich in plant debris (approximately 5%), grey-brown sandy silt (25–69 cm) with sporadic granular nodules, silty sand (69–130 cm) that gradually darkening from top to bottom, and dark sandy silt (130–160 cm) with plant debris imbedded in 150–152 cm. As shown in Fig. 2, the average contents of clay, silt, and sand fractions in core WZD are 2.51%, 69.34%, and 28.15%, respectively. The median particle size ranges between 1.96 and 6.21 Φ. Based on characteristics of the sediment profile, core WZD is divided from bottom to top into 5 zones (Fig. 2).

Moreover, after a detailed examination of both grain size and pollen records, we found no evidence of volcanic activity influencing the environmental evolution of Weizhou Island. Our sediment cores did not reveal any tephra layers, which are typically indicative of volcanic ash deposits. Similarly, there were no abrupt changes in grain size or geochemical anomalies that would suggest volcanic input (Fig. 2). Our high-resolution pollen analysis, which spans 1400 years, also did not show any shifts in vegetation composition or diversity that could be attributed to volcanic events (Fig. 3). Thus, although it is true the volcanos play an important part on the island's ecosystems, there is no recorded evidence of volcano eruption during the past 1400 years.

4.2. Chronology

The depth profile of excess ^{210}Pb and supported ^{210}Pb are displayed in Fig. S1 in the Supplementary Content. Overall, it shows a relatively steady exponential decay trend for the top 50 cm in core WZD. According to the CIC model, it reveals a sedimentation rate of ~5.3 mm/yr for the top 50 cm in the core (λ = 0.0311; Corbett and Walsh, 2015). The results of AMS ^{14}C dating and the ^{13}C/^{12}C ratio of all seven samples are shown in Table 1. An age-depth chart, drawn using R-*BACON* (Blaauw and Christen, 2011), is shown in Fig. 2. Collectively, we used the ^{210}Pb$_{ex}$ results and the median age (the red curve estimated by R-*BACON* in Fig. 2) of the radiocarbon dates to construct the chronology for core WZD. Based on R-*BACON*, the calibrated radiocarbon dates ranged from ~1400 cal yr BP to modern (Table 1). Based on the dating results, the sedimentation rate of Zones I, II, III and IV are 0.55 mm/yr, 1.01 mm/yr,

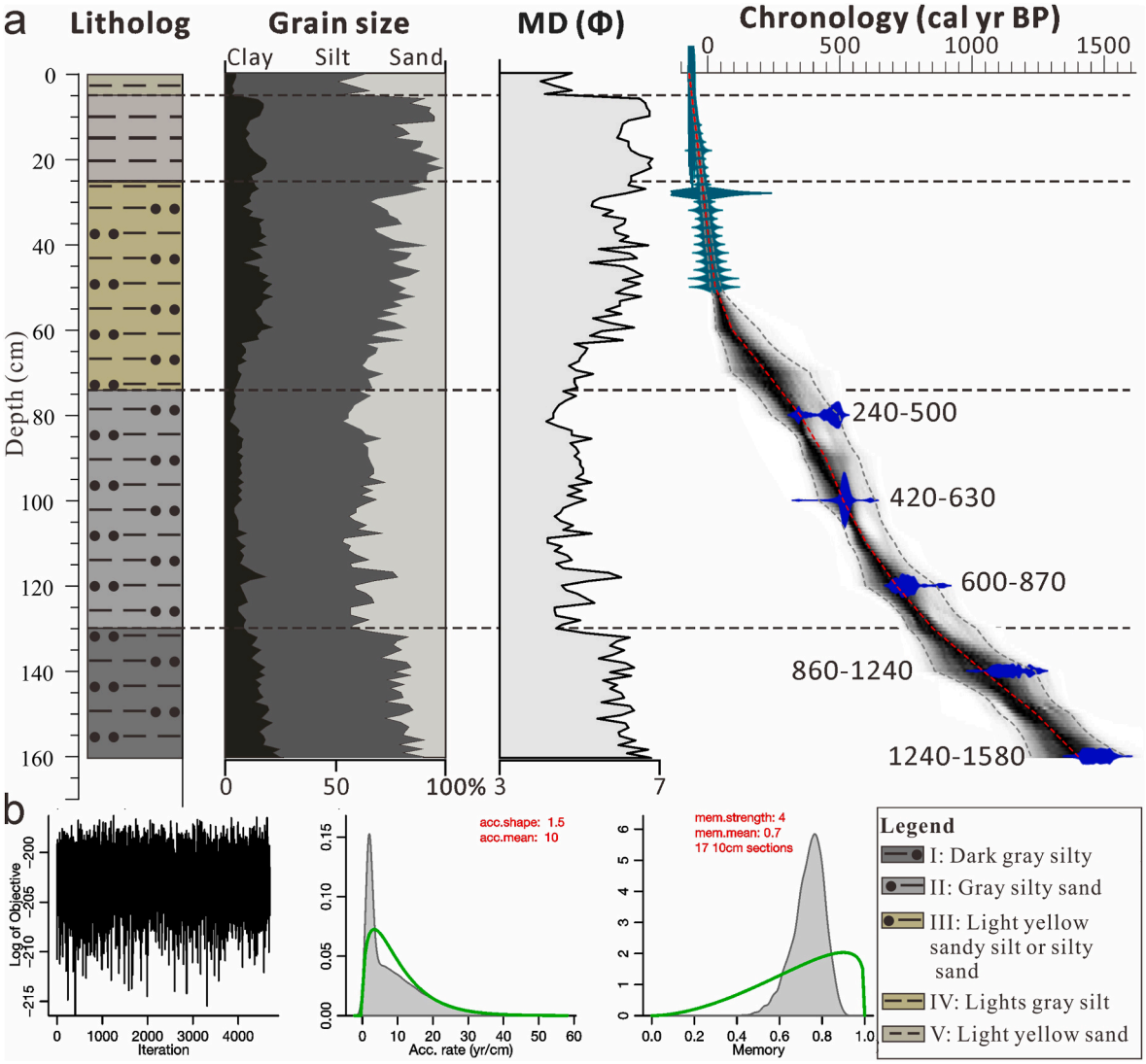

Fig. 2. Upper panel from left to right (a): Litholog, grain-size result, median particle size (Φ), and the Bayesian age-depth model for core WZD. Lower panel from left to right (b): 'Energy' of all Markov Chain Monte Carlo iterations of the run, accumulation mean and accumulation shape, and prior (green) and posterior (grey) for the memory. The age-depth model is developed by RBACON v.2.2. The red curve shows the 'best' estimated age by R-*BACON*.

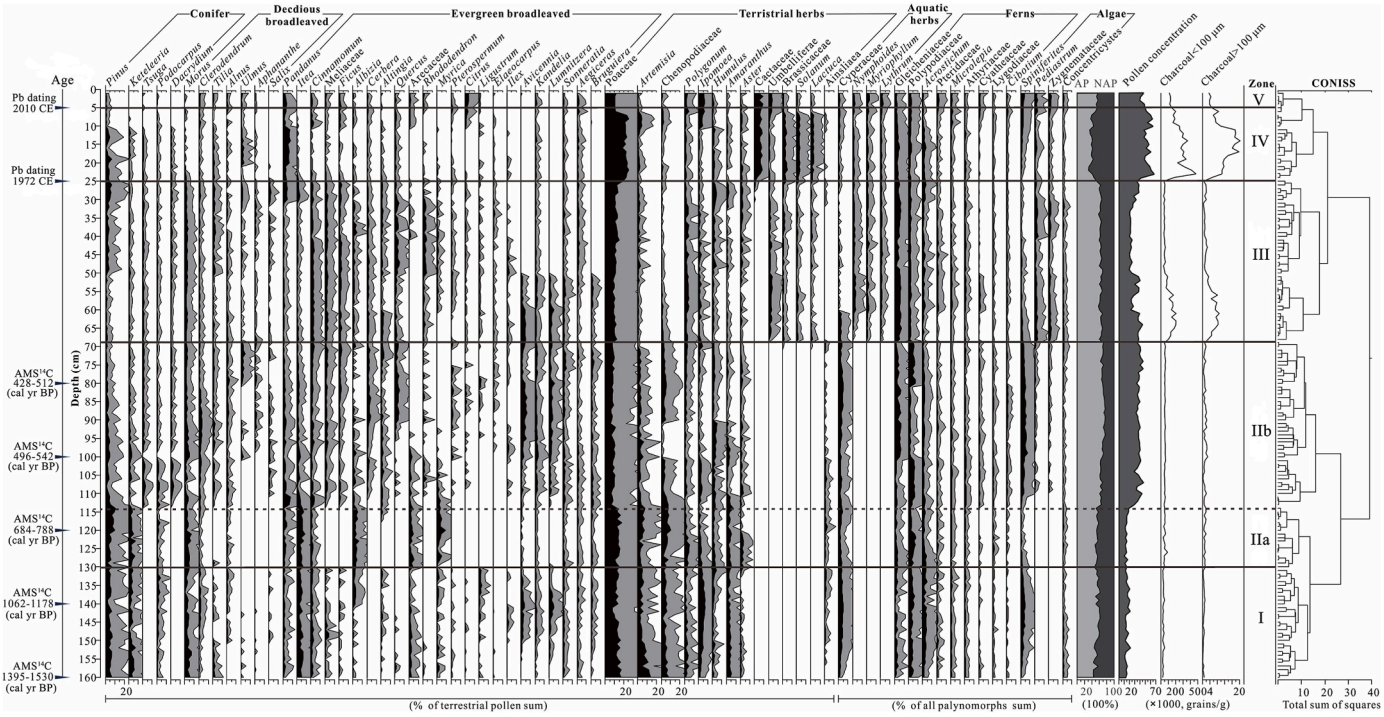

Fig. 3. Pollen diagram of core WZD (from left to right): relative frequency (%) of tree, herbaceous taxa, non-pollen palynomorphs, and concentrations of pollen and charcoal. AP and NAP marks arboreal and non-arboreal pollen taxa.

3.34 mm/yr, and 5.26 mm/yr, respectively. The calibrated range and median and weighted mean age given by the Bayesian model for each depth interval are listed in the Supplementary Content (Table S2).

4.3. Facies description based on multi-proxy analyses

Based on the 160 samples from core WZD, we identified a total of 94 pollen taxa, all of which are typical tropical-subtropical taxa. This includes 63 taxa of woody plants, 11 taxa of terrestrial herbaceous plants, 7 taxa of hydrophytic herbaceous plants, 9 taxa of fern spores, and 4 taxa of algae. Among these, the most abundant pollen taxa are woody plants like Pine (*Pinus*), with Cactaceae, Acacia, and Casuarinaceae notably concentrated in the upper half of the core. Terrestrial herbaceous plants are dominated by Poaceae (grasses), with significant contributions from Chenopodiaceae, *Artemisia*, Umbelliferae, and *Ipomoea* (Fig. 3). Aquatic plants include Cyperaceae, Polygonaceae, Lythraceae, *Nymphioides*, and *Myriophyllum* (Fig. 3). Fern spores are dominated by Gleicheniaceae and Polypodiaceae, while algae primarily consist of *Pediatrum*, Zygnetaceae, *Concentricystes*, and *Spiniferites*. Based on the grain size results, percentage and variations of major spore-pollen taxa, and the quantity of charred particles in these 160 samples, core WZD was divided into five zones from bottom to top using CONISS cluster analysis.

4.3.1. Zone I (160-130 cm, ~1400-850 cal yr BP)

This zone has a median particle size of 5.89 Φ (5.2–6.67 Φ), an average clay content of 17.26% (10.79%–26.01%), an average silt content of 62.076% (54.59%–70.1%), and an average sand content of 20.67% (9.38%–32.31%). The median particle size is the highest in the profile (Fig. 2).

This zone has the lowest spore concentration in the profile, averaging 17,678 grains/cm^3, ranging from 10,506 to 26,236 grains/cm^3 (Fig. 3). Eight samples at the core bottom (160-152 cm) contained less than 300 grains of palynomorphs. The pollen assemblages mainly consist of woody and terrestrial herbaceous taxa. Woody taxa range from 28.83% to 55.18%, with an average of 41.27%. This zone also contains some mangrove taxa (e.g., *Aegiceras*, *Kandelia*, *Avicennia*, *Sonneratia*, *Lumnitzera*, *Bruguiera*), constituting ~5.65% (2.05%–11.59%) of the total pollen sum. Other common taxa include *Pinus* (2.95%–12.31%), *Itea* (3.4%–10.96%), Arecaceae (0.38%–7.51%), *Keteleeria* (0.88%–9.3%), and others such as *Clerodendrum*, *Pandanus*, *Podocarpus*, *Tilia*, *Morus*, and Lauraceae. Terrestrial herbaceous taxa range from 18.12% to 44.03%, primarily consisting of Poaceae (9.86%–21.40%), *Artemisia* (1.66%–16.6%), Chenopodiaceae (2.63%–11.86%), *Amaranthus* (1.85%–8.58%), *Humulus*, and *Ipomoea*. Aquatic taxa are dominated by Cyperaceae at 3.85% (1.02%–6.38%). Fern spores account for 16.18% (8.59%–23.46%), mainly represented by Gleicheniaceae and Polypodiaceae. Algae are dominated by marine *Spiniferites* at 2.67% (0.33%–6.28%), with some *Concentricystes*. Charcoal particle concentration in this zone is the lowest throughout the core, primarily consisting of particles smaller than 100 μm (38,773 grains/cm^3), and larger particles averaging 841 grains/cm^3 (Fig. 3).

4.3.2. Zone II (130-69 cm, ~850-210 cal yr BP)

This zone has a median particle size of 4.86 Φ (4.21–5.94 Φ), an average clay content of 7.39% (2.84%–19.32%), an average silt content of 54.9% (46.75%–62.56%), and an average sand content of 37.71% (21.72%–46.84%). The clay content is the lowest and the sand content is the highest in this interval (Fig. 2).

The spore concentration increased significantly in this zone, ranging from 36,716 to 66,820 grains/cm^3, averaging 53,117 grains/cm^3 (Fig. 3). Woody plant taxa still dominate Zone II, slightly increasing from 41.27% in Zone I to 47.18% (37.49%–55.87%). Pine pollen slightly decreases to 3.64% (1.28%–6.51%); Arecaceae pollen disappears at 95 cm from the top; *Itea* and *Keteleeria* decrease to 2.66% and 1.78%, respectively. Pollen of *Cerbera*, *Morus*, Meliaceae, mand Lauraceae increase to 2.61%, 3.14%, 2.81%, and 2.70%, respectively. Mangrove pollen increases to 10.08% (5.50%–13.53%). Terrestrial herbaceous taxa decrease, averaging 17.85%, ranging from 12.68% to 24.32%, still primarily consisting of Poaceae (11.3%), *Artemisia* (3.55%), Chenopodiaceae (4.4%), and *Amaranthus* (2.08%), with *Humulus* slightly increasing to 3.15%. The total pollen sum of aquatic taxa slightly increases to 7.18% (3.15%–11.49%). Fern spores also increase to 20.25%

(15.54%–25.42%), with slight increase in Gleicheniaceae and Polypodiaceae, and *Cibotium* slightly rising to 1.13%. Algae increase to 7.55% (2.17%–9.98%), with occasional appearances of *Pediatrum* and Zygnetaceae, and *Spiniferites* increasing to 5.43% (1.49%–8.96%). Charcoal particle concentration rapidly increases, with particles smaller than 100 μm and larger than 100 μm averaging 54,477 grains/cm^3 and 1283 grains/cm^3, respectively (Fig. 3).

4.3.3. Zone III (69-25 cm, 210 cal yr BP – 1970 CE)

This zone has a median particle size of 5.58 Φ (4.46–6.51 Φ), an average clay content of 15.4% (8.270%–23.12%), an average silt content of 60.29% (49.66%–74.33%), and an average sand content of 24.31% (9.1%–37.24%). The clay content in Zone III is the highest throughout the core (Fig. 2).

The spore concentration slightly decreases, ranging from 25,529 to 63,295 grains/cm^3, averaging 41,403 grains/cm^3 (Fig. 3). Woody plant taxa decrease to 42.26% (22.99%–57.88%), with Pine slightly dropping to 3.51% (0.74%–8.52%). *Morus* remains stable, while Meliaceae and Lauraceae slightly rise to 3.61% and 3.59%, respectively. *Quercus* steadily appearing, constituting ~2.58% (0.58%–5.32%) of the total pollen sum. Mangrove pollen decreases to 5.78% (1.78%–11.35%). Terrestrial herbaceous taxa slightly increase to 18.07% (10.91%–29.98%), with the first appearances of Umbelliferae (1.96%), *Solanum* (0.91%), *Lactuca* (0.91%), and Brassicaceae (1.15%). Poaceae rises to 9.48% (6.44%–16.96%). *Artemisia*, Chenopodiaceae, and *Humulus* decrease to 1.62%, 1.37%, and 2.59%, respectively, with sporadic appearances of Cactaceae, *Ainsliaea*, and *Erigeron*. Aquatic taxa increase to 13.26% (6.94%–19.70%), with the first appearances of *Nymphioides*, *Myriophyllum*, and Lythraceae, rapidly increasing and reaching 2.72%, 1.98%, and 1.74%, respectively. Cyperaceae decreases and even disappears in some sample intervals. Fern spores slightly decrease to 18.63% (12.5%–27.08%), with slight increases in Gleicheniaceae and *Acrostichum* to 6.96% and 2.29%, respectively. Algae remain similar to Zone III, constituting 7.78%, with significant increases in freshwater algae like *Pediatrum* (0.98%–5.05%), Zygnetaceae (0.48%–3.64%), and marine *Spiniferites* decrease to 1.36% (0.20%–3.31%). Charcoal particle concentration continues to increase, predominantly consisting of particles smaller than 100 μm, averaging 84,952 grains/cm^3, and larger particles averaging 3237 grains/cm^3 (Fig. 3).

4.3.4. Zone IV (25-5 cm, 1970 CE –2014 CE)

This zone has a median particle size of 5.99 Φ (4.11–6.77 Φ), an average clay content of 13.88% (3.81%–19.04%), an average silt content of 72.85% (48.48%–83.40%), and an average sand content of 13.27% (2.00%–47.71%). The median particle size is the smallest; silt content is the highest; and the sand content is the lowest throughout the core (Fig. 2).

The spore concentration significantly increases, reaching the highest in the profile, at 72,662 grains/cm^3, ranging from 54,401 to 86,275 grains/cm^3 (Fig. 3). Woody plant taxa sharply decrease to 35.35% (28.06%–42.84%). Cactaceae (4.42%–12.81%) and *Pandanus* (1.8%–10.75%) significantly increase, dominating this zone. *Ulmus* and *Dimocarpus* rise to 2.02% (0.33%–5.16%) and 2.69% (0.32%–5.61%), respectively. Pine and *Quercus* slightly drop to 3.1% (0.58%–8.1%) and 1.05% (0.3%–2.52%), respectively. *Acacia* abruptly increases at 10 cm from the top, rising to 10.92%, while mangrove pollen drops to 2.82% (0.85%–5.03%). Terrestrial herbaceous taxa sharply increased to the highest level throughout the core, accounting for 29.51% (ranging from 11.93% to 42.12%) of the total pollen sum, with Poaceae being the most dominant taxon at 25.22% (14.29%–31.83%). Pollen from cultivated plants such as the *Solanum* (nightshade), *Lactuca* (lettuce), and Brassicaceae (mustard) families also increased to 3.37% (ranging from 0.71% to 5.48%), 1.98% (0.32%–5.09%), and 3.85% (1.42%–6.43%), respectively. Chenopodiaceae (goosefoot) family rises to 1.68% (0.31%–3.25%). Aquatic taxa slightly decrease to 12.54% (8.45%–22.22%). *Nymphoides* (fringed water lily), *Polygonum* (knotweed), and Umbelliferae (carrot) families decrease slightly to 2.02%, 1.62%, and 1.51%, respectively, while the Lythraceae (loosestrife) family remains stable. Fern spores decreased to 15.58% (12.60%–19.51%), while Algae remains relatively unchanged at 7.01%. Charcoal particles substantially increase, reaching their highest concentration throughout the core, with the smaller (<100 μm) and larger (≥100 μm) particles rising to 247687 grains/cm^3 and 10827 grains/cm^3, respectively (Fig. 3).

4.3.5. Zone V (5-0 cm, overwash deposits from Typhoon Rammasun in 2014)

In core WZD, a distinctive stratigraphic feature is observed in the uppermost 10 cm interval, characterized by coarser grain size materials with the highest sand fraction throughout the core. This particular sedimentary signature aligns with the characteristics of overwash storm deposits as described by Liu (2004). Since 1950, the island has experienced the impact of five major typhoons: Freda (1965), Sally (1996), Hagupit (2008), Rammasun (2014), and Mujigae (2015) (Fig. 1c). Among them, only Freda and Rammasun made directly landfall across the Island (National Oceanic and Atmospheric Administration, 2024). In particular, Rammasun is the strongest typhoon (Categories 5 on the Saffire-Simpson Scale) that ever recorded near Weizhou Island. Given the directional trajectories of these storms (Fig. 1c), a compelling case can be made for attributing the coarse sediment layer at the top of the core to the overwash deposits from Typhoon Rammasun in 2014. This assertion is predicated on the resemblance between the physical characteristics of the sediment layer and the expected geomorphological impact of Rammasun's storm surge, a hypothesis that is further substantiated by the storm's trajectory and intensity as it crossed Weizhou Island (Liu and Fearn, 1993).

4.4. Biodiversity

Palynology-based biodiversity models are used to evaluate the estimated number of pollen taxa for every sediment interval (1 cm resolution) in core WZD. The rarefied curves indicate diversity values for each sample (Fig. 4a). The estimated species richness fluctuated between 25 and 58 species per sample in 160 counted pollen samples during the past 1400 years (Fig. 4b). In our analysis of the diversity values across the five zones outlined in section 4.3, we observed significant variances in the overall estimated number of species among all pollen assemblages, as depicted in Fig. 4. Starting with Zone I, which spans from ~1400 to 850 cal yr BP (160–130 cm), it has a total of 77 taxa and 10745 counts of pollen grains. The estimated number of species *E* (Sn) showcased moderate values, ranging between 30 and 50. Transitioning to Zone II, covering ~850 to 210 cal yr BP (130–69 cm), it has a total of 81 taxa and 25491 counts of pollen grains. We noted the *E* (Sn) values initially dipped to their lowest between 28 and 43 in the 130 to 120 cm segment, before experiencing a rise to moderate values again, fluctuating between 26 and 49. Zone III, from ~210 cal yr BP to 1970 CE (69–25 cm), marked a significant shift, presenting the highest *E* (Sn) values across the entire core, with figures spanning from 50 to 60. It has a total of 90 taxa and 21416 counts of pollen grains. Moving towards the more recent past, Zone IV, which extends from 1970 to 2014 CE (25–5 cm), it has a total of 87 taxa and 8831 counts of pollen grains. The *E* (Sn) values varied from moderate to low, ranging between 40 and 57. Finally, in Zone V, from 5 to 0 cm, corresponding to the overwash deposits from Typhoon Rammasun in 2014, the *E* (Sn) values settled into a moderate range, between 45 and 55. It has a total of 71 taxa and 2598 counts of pollen grains. This fluctuation through the zones highlights the dynamic shifts in species diversity over time, reflecting the complex interplay of environmental factors influencing the pollen assemblages.

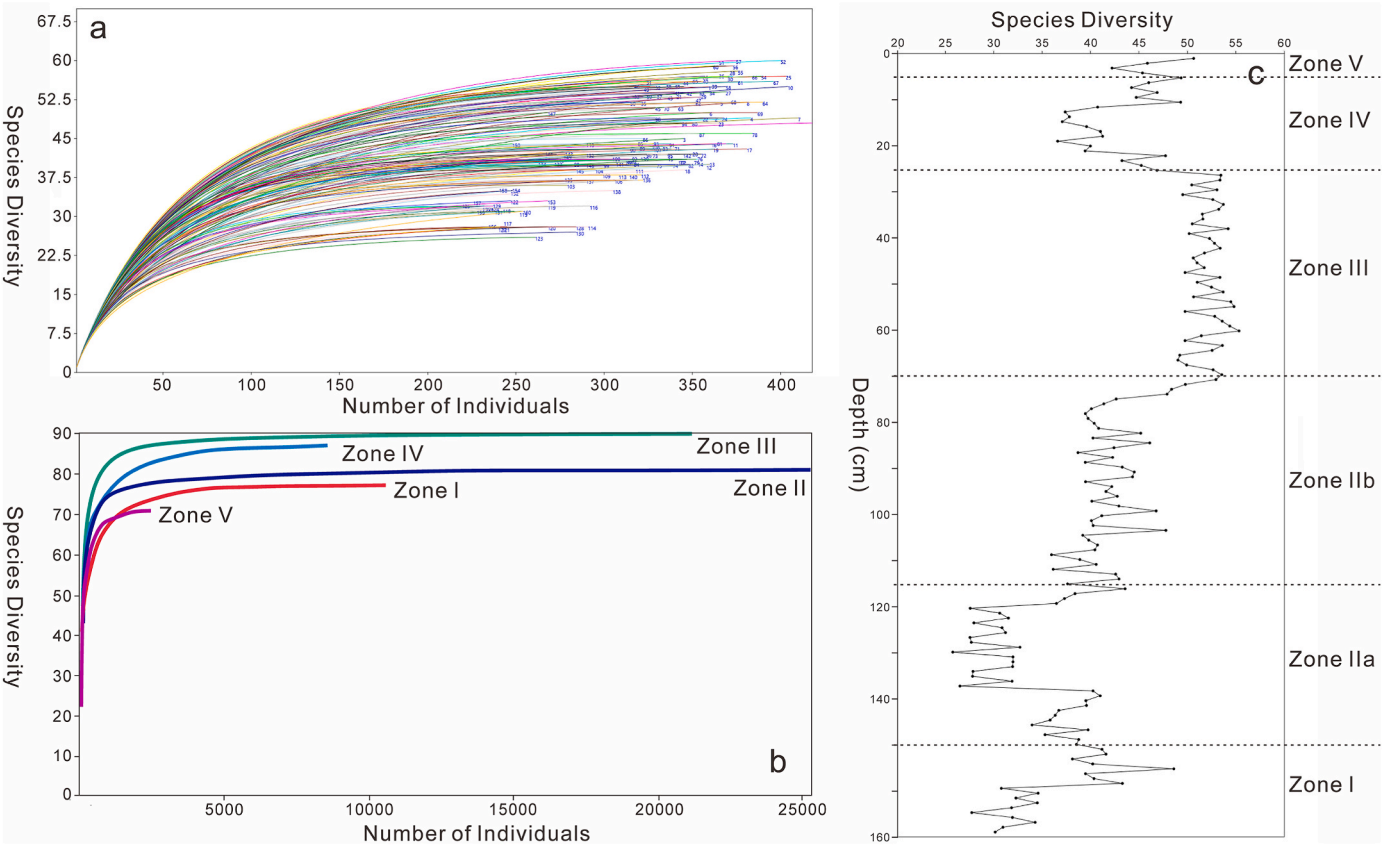

Fig. 4. Palynology-based rarefaction analysis: (a) Curves indicate estimated number of pollen taxa *E* (S_n) for every sediment interval (1 cm resolution) in core WZD, (b) estimated number of pollen taxa *E* (S_n) for each pollen zone in core WZD, (c) Palynological richness [*E* (S_n)] based on rarefaction analysis of pollen data from core WZD.

5. Discussion

5.1. Environmental fluctuation and ecosystem dynamics during the late-Holocene

Based on the multi-proxy results from core WZD, the changes in vegetation succession in the Weizhou Island over the past ~1400 years can be divided into the following four stages.

5.1.1. Marine environment under a warm and dry climate (1400-850 cal yr BP)

Prior to 850 cal yr BP, the multi-proxy characteristics of core WZD shew a clear transition from marine dominated to marine-terrestrial dominated environments. In this phase, there were fewer types of woody plant pollen taxa, with the dominant woody plants being drought-resistant species. These primarily included drought-resistant shrubs and trees, such as mulberries (*Morus* spp.) at ~5%, thorny plants of the genus *Itea* at ~6%, and palms (Arecaceae) at ~3% (Fig. 3). Additionally, drought-tolerant pines (~7%) and *Keteleeria* (~4.5%) were also found, indicating that the vegetation near the Beibu Gulf at the time was mainly seasonal rainforests, interspersed with coniferous forests. Terrestrial herbaceous taxa that adapt to a drier environment, such as Chenopodiaceae and *Amaranthus* were also found in relatively higher percentages (Cromartie et al., 2020), while hydrophilic herbaceous plants and fern spores were relatively less abundant. In addition, the sand fraction in this interval was the lowest throughout the core (Fig. 2), reflecting insufficient hydrodynamics due to the dry environment (Liu et al., 2021), while the appearance of heat-tolerant species such as *Pandanus* and *Ficus* indicates higher temperatures at the time (Fig. 3). Thus, the multi-proxy dataset indicate that the climate was relatively warm and dry during the period between 1400 and 850 cal yr BP. We believe that vegetation development on Weizhou Island was limited under a hot and dry environment, hence the pollen concentration during this stage was the lowest throughout the core.

Moreover, there was a noticeable increase in mangrove taxa around 1300-1200 cal yr BP (Fig. 3). For example, *Avicennia marina* and *Bruguiera gymnorhiza* became more abundance at ~1200 and ~1300 cal yr BP, respectively. Mangroves typically occupies the intertidal zones in the tropics and subtropics (Yu et al., 2021; 2022; 2023a). In particularly, *Avicennia* and *Bruguiera* can tolerant high salinity and are typically found on salt flats (Mo et al., 2001; Yao and Liu, 2017). Furthermore, algae were primarily dominated by *Spiniferites*, a brackish water alga generally found in nearshore marine environments (Tang et al., 2013). These microfossil characteristics indicate a marine environment in which seawater has continuously intruded into the interior of Weizhou Island. Overall, the multi-proxy dataset exhibited a landscape dominated by drought-resistant shrubs and herbs, forming a sparse woodland and grassland ecosystem (savanna), alongside a climate characterized by high temperatures and drought (Fig. 5a). We believe that during the period between 1400 and 850 cal yr BP, Weizhou Island and adjacent areas likely experienced the development of extensive coniferous forests, with species such as pine (*Pinus*) and Chinese fir (*Keteleeria fortunei*) serving as the foundational species, amidst a rising sea level.

5.1.2. Sea level low stand and transition to a humid climate (850-210 cal yr BP)

During this stage, the multi-proxy record exhibited a more dynamic environment, and this interval can be divided into two sub-stages. Between 850 and 650 cal yr BP (130-114 cm), a significant drop of mangrove taxa and marine alga (*Spiniferites*) was observed in the

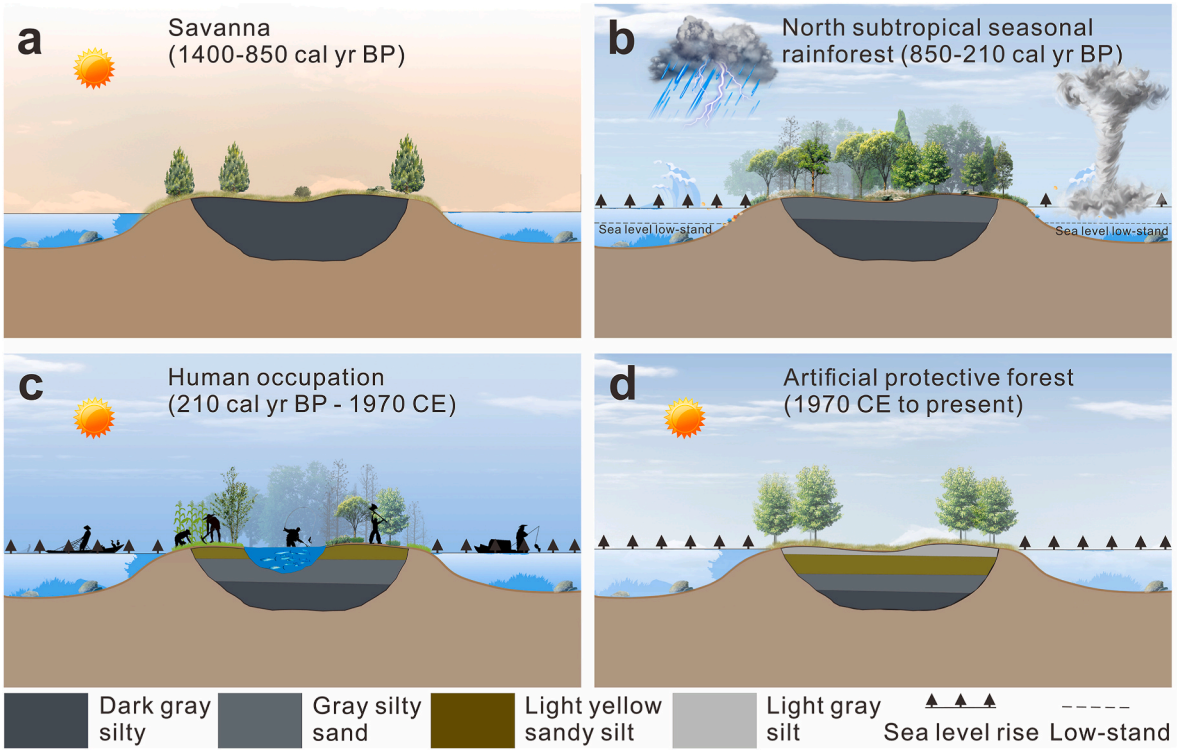

Fig. 5. Conceptual diagram illustrating the Environmental fluctuation and ecosystem dynamics on Weizhou Island since ~1400 years ago.

microfossil record, while terrestrial plants (e.g., *Myrica* and Asteraceae) increase substantially (Fig. 3). This result is in line with previous studies that documented a temporary drop of sea level at the northern South China Sea between ~850 and 670 cal yr BP (Yue and Tang, 2023), although more studies are needed to verify such sea level low stand during the late-Holocene.

After 650 cal yr BP, the types of woody plants have clearly become more diverse, and the concentration of spores has also increased during this period (Fig. 3), indicating that the vegetation coverage on the island has increased. The appearance and steady increase of temperate plants such as the *Ulmus*, Ericaceae, and *Tilia* suggest that the temperature during this period has decreased compared to the previous stage (Zone I), transitioning from a high to a mild temperature environment (Wang et al., 2019). The significant presence and dominance of *Tsuga* and *Dacrydium* suggest that mixed coniferous and broadleaf forests may have gradually developed by this time. The sharp decline and eventual disappearance of palm pollen, along with the peak values of *Salix*, Cyperaceae, and fern spores during this stage (Fig. 3), indicate a relatively humid climate (Rodrigues et al., 2022).

Moreover, the dominance of *Spiniferites* and the first appearance of marine algae, notably the diatom *Pediastrum*, a sea slug thriving in medium to deep water environments, signify that the coring site experienced a frequently submerged condition (Yao et al., 2023c). This inference is further supported by the peak sand fractions observed throughout Zone II (Fig. 2), indicative of a medium to high energy environment (Zhang et al., 2021a). Such sedimentary signature highly resembles Rammasun's storm surge deposits, as illustrated in Fig. 2, that is characterized by a distinct layering of coarse grain clastic materials. These proxy evidence provides a concrete reference that underscores a period of elevated typhoon activities near Weizhou Island. This period is marked by increased marine influence, leading to heightened sediment transport and deposition. The accumulation of coarse-grained sediments, typically linked to the strong hydrodynamic conditions of typhoons, along with the specific sedimentary features of storm surge deposits, suggests that typhoon-induced surges played a pivotal role in shaping sediment dynamics and coastal morphology around Weizhou Island during this interval (Yao et al., 2020a, 2023d). Collectively, Zone II marks a transition period where the savanna ecosystem was transforming into a typical North subtropical seasonal rainforest, indicating a shift to a mild and humid climate (Fig. 5b). Such climate facilitated the development of woody plants on Weizhou Island, laying the foundation for human occupation in the area.

5.1.3. Initiation of agriculture and transformation to a cooler climate (210 cal yr BP – 1970 CE)

During this period, plants that prefer a cooler environment consistently appear in the pollen assemblage (Fig. 3), marked by a continuous increase of Ericaceae, while *Tsuga* (hemlock) pollen remains roughly the same as in the previous phase. In particular, the frequent presence of Anacardiaceae (the cashew family), a cold-tolerant species, suggests a further decrease in temperature (Wang et al., 2019), from a mild to a cooler climate. Moreover, hydrophilic plants (e.g., Umbelliferae, *Nymphoides*, *Myriophyllum*, and *Lythrum*) and freshwater algae (e.g., *Pediastrum* and Zygnemataceae) became the dominant species (Guan, 2011). The presence of these algae, commonly found in rice fields and ditches (Tang et al., 2013), indicates the initiation of agriculture and irrigation activities, which likely resulted in the formation of small ponds or lakes. The abrupt appearance of crops and companion plants to humans, such as Brassicaceae, *Lactuca*, and *Solanum*, further proves that humans had begun rice cultivation and other agricultural practices on Weizhou Island. Several peaks of Polypodiaceae and the significant increase of charcoal fragments could be attributed to human slash-and-burn practices, leading to deforestation (Yu et al., 2021). The formation of ponds or lakes might also be related to anthropogenic activities, as the island lacks natural rivers, and humans could have created these water bodies as freshwater reservoir to sustain agricultural activities (Fig. 5c). Overall, the microfossil data shows that human occupation had significantly altered the island's original ecosystem and vegetation coverage, while the temperature has become cooler during the period between 210 cal yr BP and 1970 CE.

5.1.4. Complete ecosystem transformation due to human occupation (1970 CE – the present)

From this point forward, the significant emergence and dominance of Cactaceae on the island, particularly the extensive presence of *Acacia* pollen in recent decades, align with the characteristics of artificial protective forests along the Beihai City coastline. The increase in *Dicranopteris* spores may relate to human activities aimed at landscape transformation (Yu et al., 2021). The median grain size swiftly reduced to the finest throughout the core, accompanied by an increase in silt fraction. Field observations indicate that agricultural lands were left fallow, transitioning into wetlands, which explains the prevalence of finer materials. A continuous rise of *Spiniferites* suggests that the sea level may have been consistently rising during this period. Moreover, the pollen of woody plants initially decreased before experiencing a sharp increase, indicating a warming climate during this period (Wang et al., 2019), as evidenced by the proliferation of the tropical taxa (Fig. 3). This interval demonstrates that the island's original vegetation has been thoroughly transformed (Fig. 5d). Human activities have significantly impacted the island, coinciding with rising temperatures and continuous marine transgression.

5.2. Climatic and anthropogenic drivers of biodiversity changes on Weizhou Island over the last 1400 years

Based on the comprehensive analysis of biodiversity trends and environmental changes on Weizhou Island over the past 1400 years, it becomes evident that while multiple factors have influenced biodiversity and pollen species richness, climatic shifts emerge as the most crucial driver. These climatic changes, encompassing variations in temperature and precipitation regimes, have fundamentally shaped the ecological dynamics and vegetation patterns on the island, thereby controlling the biodiversity and pollen species richness observed in the palynological record.

5.2.1. Climatic shifts as the primary driver

Analysis of pollen species richness on Weizhou Island indicates that climatic shifts have been the primary control over ecosystem diversity and vegetation patterns throughout the last 1400 years (Fig. 6). Significant fluctuations in temperature and precipitation during this period highlight the mechanisms driving biodiversity changes on the island. This period, characterized by significant fluctuations in temperature and precipitation, highlights the fundamental mechanisms driving biodiversity changes on the island. The impact of climate on biodiversity is complex, influencing species distribution, community composition, and ecosystem function. Temperature and precipitation are critical climatic factors that directly influence the survival, reproduction, and distribution of vegetation (Lloret et al., 2012). During the earliest phase of the study period (1400-850 cal yr BP), the warm and dry climate favored drought-resistant species (Fig. 6), illustrating the direct impact of temperature and moisture availability on species composition. This period's limited biodiversity highlights the restrictive nature of arid conditions, favoring taxa adapted to withstand water stress (De Micco and Aronne, 2012).

As the climate transitioned to more humid conditions (850-210 cal yr BP), the island experienced an increase in species richness (Fig. 6). This shift underscores the role of precipitation in enhancing habitat heterogeneity, which allowed a broader array of plant taxa to thrive (Naiman et al., 2005). The development of mixed coniferous and broadleaf forests during this time reflects the influence of increased moisture availability on biodiversity, showcasing how shifts in humidity can catalyze landscape diversity. In addition, climatic shifts not only directly affect the physiological thresholds of species but also alter habitat availability and quality. Changes in climate can lead to the expansion or contraction of habitats, influencing the distribution patterns of species (Opdam and Wascher, 2004). For instance, the increase in humidity likely facilitated the expansion of wetland areas and the diversity of aquatic habitats, supporting a wider range of hydrophilic and semi-aquatic species (Fig. 6). Conversely, periods of drought and warmth may have contracted available habitats for moisture-dependent species, leading to a decrease in biodiversity.

Additionally, variations in seasonality, along with the frequency and intensity of extreme climatic events, such as typhoons and droughts,

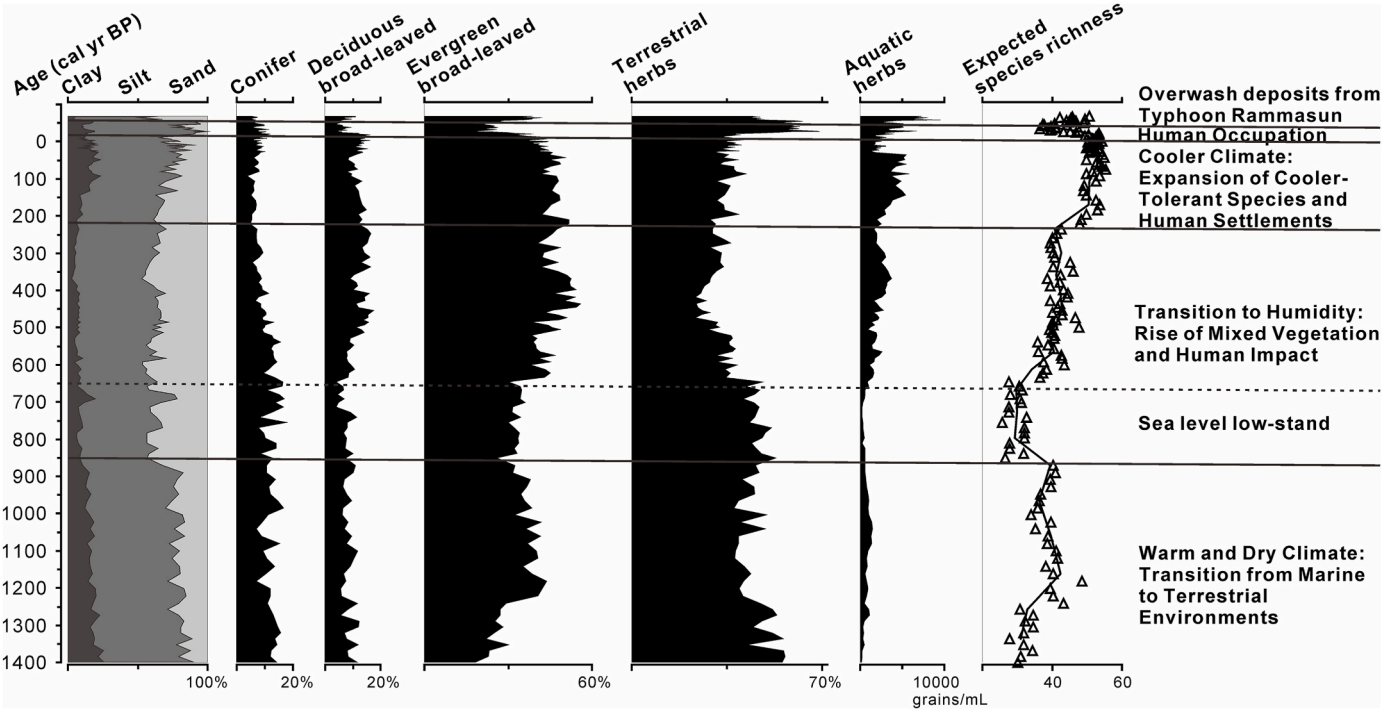

Fig. 6. Sedimentary and microfossil proxy diagram summarizing (from left to right): the inferred chronology by the Bayesian model, grain size, pollen, and rarefaction analysis results of core WZD in chronological orders.

have profound implications for biodiversity. Such events can cause immediate and drastic changes in the environment, affecting species survival and community composition (Rodrigues et al., 2021; Zhang et al., 2021b). On Weizhou Island, the occurrence of Typhoon Rammasun and its associated overwash deposits illustrates how extreme weather events, influenced by climatic conditions, can rapidly alter habitat structures and influence sediment dynamics, thereby impacting pollen deposition and species richness (Yao et al., 2023d). However, in contrast to the moderate to low pollen richness observed in Zone II, Typhoon Rammasun's overwash deposits lead to an increased E (S_n) (Fig. 6). Typhoon Rammasun, arguably the strongest landfalling typhoon ever documented near Weizhou Island, likely transported a substantial volume of marine sediments from offshore to the island's interior (Liu and Fearn, 1993; Liu, 2004). This process resulted in a pollen assemblage within the typhoon's deposits that markedly differs from the *in-situ* substrate (Fig. 4), primarily due to the inclusion of pollen transported by currents and wind from distant locations (Yao et al., 2023d). Consequently, the pollen signature associated with Typhoon Rammasun's deposits offers a regional rather than a local signal, reflecting a diverse array of sources. This phenomenon underscores the capability of significant storm events to alter local pollen deposition patterns by introducing exogenous materials, as detailed in previous study by Yao et al. (2020b). These findings emphasize the importance of considering extreme weather events when interpretating palynological records, as such events can significantly influence perceived biodiversity and environmental conditions.

Furthermore, long-term climatic trends, including gradual warming or cooling and changes in precipitation patterns, shape landscape diversity and vegetation succession (Willis and MacDonald, 2011). These trends influence species migration, adaptation, and extinction rates, thereby affecting biodiversity over time. The adaptation and migration of tropical taxa in response to warming conditions in the most recent phase (1970 CE – present) highlight the successional responses of vegetation to climate change (Fig. 6), further emphasizing climate's role as a primary driver of biodiversity on an isolated small island setting. In summary, climatic shifts, through their direct and indirect effects on temperature, precipitation, habitat availability, and the frequency of extreme events, emerge as the primary control over biodiversity and pollen species richness on Weizhou Island. These climatic factors not only dictate the immediate survival and distribution of species but also drive long-term ecological and vegetation successional processes, shaping the island's landscape diversity over the past 1400 years.

5.2.2. Human activities and environmental changes

Human activities and their consequent environmental changes have also significantly influenced the biodiversity and pollen species richness on Weizhou Island. While climatic shifts are the primary driver, anthropogenic interventions-especially agriculture, deforestation, and urbanization-provide a complex secondary influence on the island's ecological dynamics.

The initiation of agriculture on Weizhou Island, particularly during the cooler climate phase (210 cal yr BP to 1970 CE), marked a significant anthropogenic alteration of the natural landscape (Fig. 6). Converting native vegetation to agricultural lands changed the physical landscape and introduced new plant species into the ecosystem, both as crops and associated weeds (Fig. 3). This transformation led to an increase in habitat heterogeneity, providing niches for a wider array of species and thereby influencing species richness. The presence of agriculture indicated by pollen from cultivated plants and associated species suggests a diversification of the plant community in response to human cultivation practices. The expansion of agricultural activities often came at the expense of natural forests, leading to deforestation and significant alterations in the island's vegetation cover (Ramankutty et al., 2006). Deforestation for agriculture, settlement expansion, or as part of slash-and-burn practices, reduced the area covered by native forests, impacting the habitats available for various pioneer species and thus affecting biodiversity (Vieira et al., 2008). The significant increase in charcoal fragments (Fig. 7), indicative of slash-and-burn practices, points to human-induced disturbances that likely facilitated the colonization of various weeds, which could temporarily increase species richness but might have long-term negative effects on ecosystem stability and resilience (Rodrigues et al., 2022; Yao et al., 2023b).

In recent decades, Weizhou Island has experienced increased urbanization and infrastructure development, particularly over the past 80 years with significant migration to the island (Qi et al., 2003; Zhu et al., 2012). This development has led to further landscape transformation, with natural habitats being replaced by built-up areas. Urbanization processes typically reduce habitat size and connectivity, leading to a decline in biodiversity (McDonald et al., 2013). However, urban areas can also create microhabitats for certain species (Lundholm and Marlin, 2006), potentially contributing to an increase in pollen species richness observed in certain segments of the core (Fig. 6). In particular, the initiation of the Weizhou Island Wetland Ecological Restoration Project in 2012, under the auspices of the regional nature reserve in Guangxi, has led to significant restoration efforts, particularly in areas like the Niujiaokeng wetland, which now serves as a sanctuary for migratory birds and represents the island's largest intermittent freshwater wetland (Zhang et al., 2018). The impact of urbanization on biodiversity is complex, involving both losses in native species and gains in non-native, often invasive, species.

In addition, the development of irrigation systems for agriculture introduced new water bodies into the landscape, such as ponds and lakes, which were not naturally present on the island. These anthropogenic water bodies altered the island's hydrological dynamics, potentially supporting a different set of aquatic and semi-aquatic species. The increase in hydrophilic plants and freshwater algae in the pollen record likely reflects these changes (Fig. 6), indicating how human alteration of water systems has influenced biodiversity. In conclusion, human activities, particularly agriculture, deforestation, urbanization, and water management, have played a crucial role in shaping the biodiversity and pollen species richness on Weizhou Island. These anthropogenic changes have both directly and indirectly influenced the ecological dynamics of the island, altering habitat structures, introducing new species, and changing the landscape in ways that have profound implications for biodiversity. While climatic shifts are the primary driver of biodiversity changes, the impact of human activities highlights the interconnectedness between natural and anthropogenic factors in shaping landscape diversity and vegetation succession. Understanding these interactions is crucial for developing effective conservation and management strategies that balance human needs with the preservation of natural vegetation.

5.2.3. Global significance and Uniqueness of biodiversity changes on Weizhou Island

The multi-proxy dataset from Weizhou Island significantly enhance our understanding of how climatic and anthropogenic factors influence island biodiversity globally. This study stands out in the palynological literature due to its high resolution, with 160 pollen samples covering the past 1400 years, providing data at less than 10-year intervals. This temporal resolution is exceptionally high compared to most palynological studies, offering a detailed and continuous record of ecological changes. Unlike typical ecological monitoring studies that span only a few decades at maximum, this long-term study captures extensive historical and prehistorical environmental shifts, making it a valuable resource for understanding long-term biodiversity dynamics.

Comparative studies from other island ecosystems, such as the Galápagos and Hawaiian Islands, have used various methods to document ecological changes, including short-term ecological monitoring, remote sensing, and genetic studies. For example, El Niño's impact on the Galápagos has been studied using remote sensing to observe changes in vegetation (Trueman and d'Ozouville, 2010), while in Hawaiian, vegetation changes have been monitored through periodic ecological surveys (Zimmerman et al., 2007). These studies, although insightful, often lack the long-term perspective provided by high-resolution

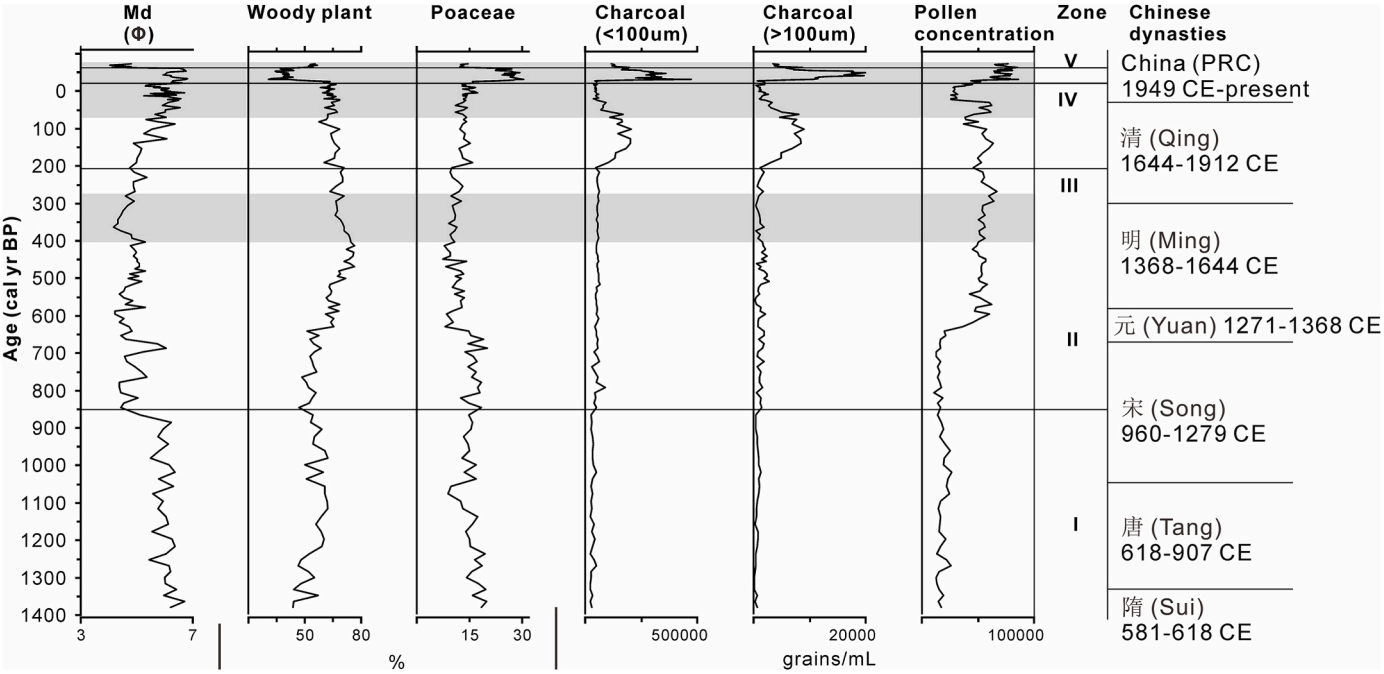

Fig. 7. Human impact on the island across seven Chinese dynasties (from left to right): Median particle size (Φ), woody and herbaceous plant pollen content, concentrations of both large and small charcoal particles, and overall Poaceae concentration. The shaded sections mark the intervals with strong human activities derived from historical documents.

palynological records. In comparison, this Weizhou Island pollen record reveals how climatic shifts, particularly variations in temperature and precipitation, have driven biodiversity changes over a millennial time scale. This study also underscores the impact of human activities such as agriculture, deforestation, and urbanization on the island's ecological dynamics. Similar anthropogenic impacts have been observed in Madagascar, where deforestation and the introduction of non-native species have significantly altered biodiversity (Harper et al., 2007). In addition, studies from the Caribbean revealed that historical land use changes have led to declines in endemic species (Smith et al., 2012). However, the unique combination of high-resolution temporal data and long-term scope in our study provides a more detailed understanding of these influences.

In sum, the insights from Weizhou Island have broader implications for global conservation efforts. Islands in tropical and subtropical regions are often biodiversity hotspots and understanding the factors driving the ecological changes on these islands is crucial for effective conservation strategies. Additionally, our record highlights the importance of integrating long-term climatic and palynological data in biodiversity assessments, providing a unique baseline dataset that can enhance our understanding of the resilience of island ecosystems to future environmental changes (Bellard et al., 2014).

5.3. *The history of human activities across seven Chinese dynasties inferred from multi-proxy record and historical documents*

Pollen from cultivated plants, such as weeds and cereal crops, serves as a valuable indicator of human activities and their influence on ecosystem dynamics (Li et al., 2008). Previous research indicatess that Poaceae and Brassicaceae pollen are effectively markers of human activities (Shu et al., 2007). Charcoal particles serve as indicators of fire events, with large particles ($D \geq 100$ μm) indicating intense slash-and-burn practices, and smaller particles ($D < 100$ μm) indicating local wildfires (Li et al., 2006; Liu, 2019; Wang et al., 2020). This study infers the history of ancient human activities on Weizhou Island and their association with climatic and environmental fluctuations across different Chinese dynasties, using historical documents, median particle size from core WZD, concentrations of large and small charcoal particles, woody and herbaceous plant pollen content, and Poaceae pollen content (Fig. 7).

5.3.1. *Sui Dynasty (581–618 CE) to Song Dynasty (960–1279 CE)*

During this period, both charcoal and species diversity were at their lowest levels throughout the core, indicating minimal human activity. This is supported by the pollen analysis, which shows no presence of Brassicaceae pollen and a low content of Poaceae pollen (Fig. 3). However, the historical document 'Records of Jiaozhou' by Liu Xinqi mentions that "On Weizhou Island, there is a stone chamber, inside which a stone resembles the shape of a drum. A pomegranate stick leans against the stone wall, and pearl divers often worship it" (Liu, 1992; Zhu et al., 2012). This suggests that Weizhou Island was visited by pearl divers as early as the Jin Dynasty (266–420 CE, 1530–1684 cal yr BP), but they did not formally settle there. The overall climate of Weizhou Island during this period was hot and dry, which was not ideal for human habitation, resulting in minimal human impact on the island. The high temperatures and dry conditions likely contributed to the occurrence of natural fires, with the charcoal from this stage likely resulting from local wildfires, leaving Weizhou Island largely in its original ecological state (Fig. 7).

5.3.2. *Song to Ming Dynasty (1368–1644 CE)*

Aside from the period of sea level low stand (~850 and 670 cal yr BP), this interval was warmer and more humid than the previous one, making it more suitable for human occupation. According to microfossil and non-pollen palynomorphs analysis (Fig. 3), the concentration of charcoal particles remained low in this section, indicating a low probability of wildfires on the island. However, consistent Poaceae content, along with increased woody plant pollen and decreased herbaceous pollen (Fig. 7), suggests that the vegetation was not significantly affected by human activity and that shrubland gradually became the dominant ecosystem on the island. This period likely laid the foundation for later human settlement on the island, with an increase in wood availability for burning, warmer and more humid climate, and the succession of the island's vegetation facilitating human habitation.

5.3.3. Ming to Qing Dynasty (1644–1912 CE)

Historical documents indicate that farmers began migrating and cultivating land on Weizhou Island since 1578 CE (372 cal yr BP) (Zhu et al., 2012), marking the first instance of prolonged human habitation. At approximately the same time, our pollen record documented the emergence of Brassicaceae (mustard and cabbage) and *Lactuca* (lettuce) pollen, among other agricultural crop pollens (Fig. 3), indicates a significant increase in agricultural activities on Weizhou Island. As depicted in Fig. 7, a surge in charcoal and Poaceae pollen content from ~210 cal yr BP serves as additional evidence, indicating the beginning of rice cultivation, a staple in Chinese households and cuisine. A decline in woody plant pollen suggests increased human use of wood for burning, reflecting widespread slash-and-burn practices on Weizhou Island. Moreover, a significant increase in aquatic plants, such as *Lythrum* and *Myriophyllum*, was observed in the pollen record (Fig. 3). This microfossil signature suggests that, due to the absence of natural water reservoirs on the island (Deng et al., 2017), humans began constructing ponds and lakes for water storage. This allowed for aquaculture in these man-made water bodies while engaging in fishing activities, hence a surge in aquatic plant.

The corresponding period saw a noticeable trend towards finer median particle sizes, likely related to fishing and agriculture activities under primitive living conditions (Zhu et al., 2012), leading to a more enclosed sedimentary environment with reduced material sources and finer sediments (Fig. 2). In later periods, our coring area was likely used as farmlands, causing sediment disturbance and turnover due to ploughing, with continuous changes in median particle sizes (Fig. 7), indicating the impact of human activities on the sedimentary environment of Weizhou Island. The sedimentary changes occurring on Weizhou Island during this stage had become the result of both natural and human factors. Around 1960 CE, Cactaceae (*Cactus*) first appeared, pointing to international trade routes and cultural exchanges between China and other regions, as cacti are native to foreign regions (He, 2012). Moreover, From the first year of Emperor Kangxi (1662 AD) to the eleventh year of Emperor Jiaqing (1806 AD), the residents of Weizhou Island were forced to relocate to the mainland three times, and the island's administrative organization was abolished (Zhu et al., 2012). During this period, fluctuations in large charcoal particles ($D \geq 100$ μm) and median particle sizes likely resulted from demographic changes.

5.3.4. Modern era (1949 CE to the present)

This stage marked the most thorough transformation of the original vegetation, characterized by a rapid decrease in forest taxa and an increase in herbaceous plants. Both sizes of charcoal particles and Poaceae pollen sharply rose to the highest levels observed in the entire sediment profile, and the median particle size rapidly became finer, indicating unprecedented intense human activity. According to historical document, there were already 400 people settled on Weizhou Island by 1860 CE (Peng, 2012). A few years later (1867 CE), the emperor of Qing Dynasty lifted the island's ban, relocating farmers from Leizhou and Lianzhou to the island, leading to the revival of Weizhou Island's fields and cottages that had been deserted for hundreds of years (Liao et al., 2012). Continuous expansion and reckless deforestation had a tremendous impact on the original vegetation. According to "The Annals of Weizhou Island" (Zhu et al., 2012), before 1949 CE, Weizhou Island was essentially a barren island without forests. Apart from some elm trees, spiky bamboo, and longan trees around the villages, the island was covered with sparse short grass, and dew grass. The settlers relied on grass roots, crop stalks for fuel, and supplies from the mainland for timber and fuel for maritime activities. After 1949 AD, an artificial forest landscape was formed on Weizhou Island, primarily consisting of *Casuarina equisetifolia* and *Acacia*, complemented by camphor and neem trees for protection. In the secondary natural vegetation, succulent and spiny cacti, particularly widespread across the island (Zhu et al., 2012), matched the pollen records of the last 50 years in this study, showing that cacti had become a dominant plant on the island, along with camphor, neem, *Casuarina equisetifolia*, and *Acacia*, creating a unique vegetation landscape of Weizhou Island. According to government document, it wasn't until the mid-1980s that China began systematically developing *Casuarina equisetifolia* plantation in provinces and regions along the coast, such as Guangxi (Zhong et al., 2005). Since the 1960s, China has introduced the *Acacia* tree, which has been widely planted in southern provinces like Guangxi (Lu et al., 2004). The impact of human activities on Weizhou Island during this period was profound. Despite an increase in precipitation, woody plants did not continue to increase, and humans introduced plants that had never appeared on Weizhou Island prevailed, completely altering its landscape.

5.3.5. Global context and Comparative analysis of long-term Ecosystem Changes

Comparing our dataset with other studies from islands of similar size reveals significant similarities and differences. In the Mediterranean, high-resolution pollen records have documented how ancient civilizations like the Romans and Greeks impacted their landscapes through agriculture and urbanization, leading to significant vegetation shifts (Mercuri et al., 2011). Similarly, on Easter Island, pollen records have shown how deforestation and agricultural practices by ancient Polynesians led to ecological collapse (Mann et al., 2008). These findings resemble our record from Weizhou Island, where agricultural intensification during the Ming to Qing Dynasties (1644–1912 CE) transformed the ecosystem similarly. However, unlike Easter Island, where deforestation led to ecological decline, Weizhou Island experienced both degradation and adaptation, highlighting different outcomes of human-environment interaction.

Our study also contrasts with the long-term ecological changes observed in the North Atlantic islands, such as Iceland and Greenland, where Norse settlements significantly altered the landscape through grazing and farming (Vésteinsson et al., 2002). These regions experienced severe soil erosion and vegetation loss, similar as the deforestation observed on Weizhou Island. However, the adaptation strategies on Weizhou Island, including the construction of ponds and the introduction of new crops, demonstrate a unique response to environmental pressures, differing from the more homogenous impacts seen in the North Atlantic. Therefore, the insights from Weizhou Island underscore the importance of integrating high-resolution, long-term data in better understanding the complex dynamics between natural and human factors.

6. Conclusion

Our high resolution (sub-decadal) pollen record of the late-Holocene ecological and environmental dynamics on Weizhou Island has meticulously illustrated the transformation of its ecosystem through four pivotal stages, each marked by distinct climatic and anthropogenic influences. These stages offer a window into the complex interaction between natural processes and human activities that have altered the island's biodiversity over approximately the last 1400 years, as summarized below.

- **Initial Stage** (1400-850 cal yr BP):

  Climate: Warm and dry.
  Ecosystem: Savanna-like, dominated by drought-resistant species.
  Human Impact: Minimal, inferred from sparse pollen and sedimentary data.
  Historical Records: Scant, aligning with minimal archaeological evidence.

- **Second Stage** (850-210 cal yr BP):

  Climate: Shift to humid conditions.

Ecosystem: Development of North subtropical seasonal rainforest.
Biodiversity: Significant increase in vegetation diversity.
Human Activities: Early agricultural endeavors detailed in historical documents, reflected in enhanced biodiversity.

- **Third Stage** (210 cal yr BP to 1970 CE):

Climate: Cooler.
Human Activities: Advent of agriculture and aquaculture, extensive landscape modification through slash-and-burn practices and water management systems.
Ecosystem Changes: Dramatic alterations in flora composition and introduction of crop species.
Historical Correlation: Thoroughly documented, highlighting significant human impact on biodiversity and landscape diversity.

- **Final Stage** (1970 CE to Present):

Transformation: Diverse ecosystem replaced by artificial protective forests.
Human Influence: Dominant, with landscape now characterized by anthropogenic biomes.
Documentation: Well-documented in environmental records and historical literature, signifying culmination of centuries of human influence.

The significance of our study lies in its holistic approach, integrating paleoecological data with historical narratives to understand the dynamic interactions between climatic shifts, human activities, and biodiversity changes. This integration reveals the history of Weizhou Island's environmental transformations, highlighting the resilience and vulnerability of island ecosystems to external pressures. Future research should incorporate interdisciplinary methods, such as geochemical analyses and detailed archaeological investigations, to further refine our understanding of human-environment interactions. Exploring the socio-economic drivers behind historical land-use changes could provide deeper insights into the drivers and consequences of human modifications. Additionally, examining contemporary challenges like climate change and urbanization in the context of the island's long history of adaptation could offer valuable lessons for sustainable management and conservation strategies in similar ecological settings worldwide.

CRediT authorship contribution statement

Yuanfu Yue: led the project and assisted in writing and editing. **Xi Xiang:** led the multi-proxy analysis. **Dan Zhao:** led the graphic design. **Shixiong Yang:** assisted in writing and editing. **Qiang Yao:** conceived the hypothesis, lead the numeric analysis, and wrote the manuscript.

Declaration of competing interest

The authors declare that they have no known competing financial interests or personal relationships that could have appeared to influence the work reported in this paper.

Data availability

Data will be made available on request.

Acknowledgments

This study was jointly funded by the National Natural Science Foundation of China (Grants Nos. 42366002, 41702182), the Guangxi Scientific Projects (Grant No. 2018GXNSFAA281293), and Ocean Negative Carbon Emissions Program.

Appendix A. Supplementary data

Supplementary data to this article can be found online at https://doi.org/10.1016/j.quascirev.2024.108977.

References

Bakker, J.P., Baas, A.C., Bartholdy, J., Jones, L., Ruessink, G., Temmerman, S., van de Pol, M., 2016. Environmental impacts-coastal ecosystems. In: North Sea Region Climate Change Assessment. Springer International Publishing, Cham, pp. 275–314, 275-314.
Barbier, E.B., 2015. Valuing the storm protection service of estuarine and coastal ecosystems. Ecosyst. Serv. 11, 32–38.
Bellard, C., Cassey, P., Blackburn, T.M., 2014. Alien species as a driver of recent extinctions. Biol. Lett. 10 (2), 20130970.
Birks, H.J.B., Line, J.M., 1992. The use of rarefaction analysis for estimating palynological richness from quaternary pollen-analytical data. Holocene 2, 1–10.
Blaauw, M., Christen, J.A., 2011. Flexible paleoclimate age-depth models using an utoregressive gamma process. Bayesian Analysis 6, 457–474.
Chang, C.C., Turner, B.L., 2019. Ecological succession in a changing world. J. Ecol. 107 (2), 503–509.
Corbett, D.R., Walsh, J.P., 2015. 210 lead and 137 cesium. Handbook of Sea-Level Research. John Wiley & Sons, Ltd. https://doi.org/10.1002/9781118452547.ch24.
Colinvaux, P.A., Schofield, E.K., 1976. Historical ecology in the galapagos islands: I. A Holocene pollen record from El junco lake, isla san cristobal. J. Ecol. 64 (3), 989–1012.
Corenblit, D., Steiger, J., 2009. Vegetation as a major conductor of geomorphic changes on the Earth surface: toward evolutionary geomorphology. Earth Surf. Process. Landforms 34 (6), 891–896.
Cromartie, A., Blanchet, C., Barhoumi, C., Messager, E., Peyron, O., Ollivier, V., Sabatier, P., Etienne, D., Karakhanyan, A., Khatchadourian, L., Smith, A.T., 2020. The vegetation, climate, and fire history of a mountain steppe: a Holocene reconstruction from the South Caucasus, Shenkani, Armenia. Quat. Sci. Rev. 246, 106485.
De Micco, V., Aronne, G., 2012. Morpho-anatomical Traits for Plant Adaptation to Drought. Plant Responses to Drought Stress: from Morphological to Molecular Features. Springer Berlin Heidelberg, Berlin, Heidelberg, pp. 37–61.
De Steven, D., Toner, M.M., 2004. Vegetation of upper coastal plain depression wetlands: environmental templates and wetland dynamics within a landscape framework. Wetlands 24 (1), 23.
Deng, S., Li, M., Sun, H., Chen, Y., Qu, L., Zhang, X., 2017. Exploring temporal and spatial variability of precipitation of Weizhou island, south China sea. J. Hydrol.: Reg. Stud. 9, 183–198.
Doney, S.C., Ruckelshaus, M., Emmett Duffy, J., Barry, J.P., Chan, F., English, C.A., Galindo, H.M., Grebmeier, J.M., Hollowed, A.B., Knowlton, N., Polovina, J., 2012. Climate change impacts on marine ecosystems. Ann. Rev. Mar. Sci 4, 11–37.
FitzGerald, D.M., Hughes, Z., 2019. Marsh processes and their response to climate change and sea-level rise. Annu. Rev. Earth Planet Sci. 47, 481–517.
Ge, Q.S., Zhu, H.Y., 2021. Changes of the physical and human geographical environment in China during the past 2000 years. Acta Geograph. Sin. 76 (1), 3–14 (in Chinese).
Guan, Z., 2011. Pollen Morphology of Common Aquatic Vascular Plants in China. Science Press, Beijing, pp. 1–157.
Hammer, Ø., Harper, D.A., 2001. Past: paleontological statistics software package for educaton and data anlysis. Palaeontol. Electron. 4 (1), 1.
Harper, G.J., Steininger, M.K., Tucker, C.J., Juhn, D., Hawkins, F., 2007. Fifty years of deforestation and forest fragmentation in Madagascar. Environ. Conserv. 34 (4), 325–333.
Harley, C.D., Randall Hughes, A., Hultgren, K.M., Miner, B.G., Sorte, C.J., Thornber, C.S., Rodriguez, L.F., Tomanek, L., Williams, S.L., 2006. The impacts of climate change in coastal marine systems. Ecol. Lett. 9 (2), 228–241.
He, J., 2012. Exotic Plants in China. Shanghai Science and Technology Press, pp. 1–724 (in Chinese).
He, Q., Silliman, B.R., 2019. Climate change, human impacts, and coastal ecosystems in the Anthropocene. Curr. Biol. 29 (19), R1021–R1035.
Jacobson, G.L., Bradshaw, R.H., 1981. The selection of sites for paleovegetational studies 1. Quat. Res. 16 (1), 80–96.
Jackson, J.B., Kirby, M.X., Berger, W.H., Bjorndal, K.A., Botsford, L.W., Bourque, B.J., Bradbury, R.H., Cooke, R., Erlandson, J., Estes, J.A., Hughes, T.P., 2001. Historical overfishing and the recent collapse of coastal ecosystems. Science 293 (5530), 629–637.
Kim, D., Cairns, D.M., Bartholdy, J., 2011. Wind-driven sea-level variation influences dynamics of salt marsh vegetation. Ann. Assoc. Am. Geogr. 101 (2), 231–248.
Kirwan, M.L., Megonigal, J.P., 2013. Tidal wetland stability in the face of human impacts and sea-level rise. Nature 504 (7478), 53–60.
Li, X., Z, X., Xue, S., Dodsib, J., 2006. Different size method of charcoal analysis in loess and its significance in the study of fire variation. J. Lake Sci. 18 (5), 540–544 (in Chinese).
Li, Y., Zhou, L., Cui, H., 2008. Pollen indicators of human activity. Chin. Sci. Bull. 53 (9), 1281–1293.
Liang, J.Y., Wan, Q.L., 1995. Study on the variation law of SST in the South China Sea and its impact on China's climate. South China Sea Research and Development 95 (4), 3–14 (in Chinese).

Liao, Q.X., You, M.S., Liu, X., 2012. Analysis on climate change characteristics of Weizhou Island offshore in recent 30 years. Journal of Meteorological Research and Application 33 (S1), 140–141 (in Chinese).
Liu, C., Tang, Q., Qiao, S., 2021. Influencing factor analysis of median grain size distribution in sediment from the Yellow Sea based on geodetector. Adv. Mar. Sci. 39 (4), 591–600 (in Chinese).
Liu, K.B., 2004. Paleotempestology: principles, methods, and examples from Gulf Coast lake sediments. Hurricanes and typhoons: past, present, and future 13, 57.
Liu, K.B., Fearn, M.L., 1993. Lake-sediment record of late Holocene hurricane activities from coastal Alabama. Geology 21 (9), 793–796.
Liu, L., 2019. The natural fire history during warming periods of Cenozoic. Quat. Sci. 39 (5), 1289–1296 (in Chinese).
Liu, W., Yu, K., Wang, R., Yan, T., 2020. Uranium-series ages of Beigang beachrock at WeizhouIsland and their significance in recording sea level variation. Quat. Sci. 40 (3), 764–774. https://doi.org/10.11928/j.issn.1001-7410.2020.03.14 (in Chinese).
Liu, X.Q., 1992. Records of Jiaozhou. Beijing Bibliographic Literature Publishing House, pp. 1–1776 (in Chinese).
Lloret, F., Escudero, A., Iriondo, J.M., Martínez-Vilalta, J., Valladares, F., 2012. Extreme climatic events and vegetation: the role of stabilizing processes. Global Change Biol. 18 (3), 797–805.
Lu, D.D., Wu, B.G., Wang, X.Q., Zheng, L., Jia, Y.G., 2004. A general review on the research development of Acacia spp. Journal of Fujian College of Forestry 24 (1), 92–96 (in Chinese).
Lundholm, J.T., Marlin, A., 2006. Habitat origins and microhabitat preferences of urban plant species. Urban Ecosyst. 9, 139–159.
Mann, D., Edwards, J., Chase, J., Beck, W., Reanier, R., Mass, M., et al., 2008. Drought, vegetation change, and human history on Rapa Nui (Isla de Pascua, Easter Island). Quat. Res. 69 (1), 16–28.
Maiti, K., Carroll, J., Benitez-Nelson, C.R., 2010. Sedimentation and particle dynamics in the seasonal ice zone of the Barents Sea. J. Mar. Syst. 79 (1–2), 185–198.
McDonald, R.I., Marcotullio, P.J., Güneralp, B., 2013. Urbanization and Global Trends in Biodiversity and Ecosystem Services. Urbanization, Biodiversity and Ecosystem Services: Challenges and Opportunities: a Global Assessment, pp. 31–52.
Mercuri, A.M., Sadori, L., Uzquiano Ollero, P., 2011. Mediterranean and north-African cultural adaptations to mid-Holocene environmental and climatic changes. Holocene 21 (1), 189–206.
Mo, Z.C., Fan, H.Q., He, B.Y., 2001. Effects of seawater salinity on hypocotyl growth in two mangrove species. Acta Phytoecol. Sin. 25 (2), 235–239 (in Chinese).
Naiman, R.J., Bechtold, J.S., Drake, D.C., Latterell, J.J., O'Keefe, T.C., Balian, E.V., 2005. Origins, patterns, and importance of heterogeneity in riparian systems. Ecosystem Function in Heterogeneous Landscapes, pp. 279–309.
National Oceanic and Atmospheric Administration (NOAA), Historical Hurricane Tracks. Retrieved January 26, 2024, from https://coast.noaa.gov/hurricanes/#map=4/32/-80.
Nienhuis, J.H., Kim, W., Milne, G.A., Quock, M., Slangen, A.B.A., Törnqvist, T.E., 2023. River deltas and sea-level rise. Annu. Rev. Earth Planet Sci. 51, 79–104.
Nwipie, G.N., Hart, A.I., Zabbey, N., Sam, K., Prpich, G., Kika, P.E., 2019. Recovery of infauna macrobenthic invertebrates in oil-polluted tropical soft-bottom tidal flats: 7 years post spill. Environ. Sci. Pollut. Control Ser. 26, 22407–22420.
Opdam, P., Wascher, D., 2004. Climate change meets habitat fragmentation: linking landscape and biogeographical scale levels in research and conservation. Biol. Conserv. 117 (3), 285–297.
Palynology Group of Paleobotany Research Office, Beijing Institute of Botany, Chinese Academy of Sciences, 1976. Spore Morphology of Chinese Ferns. Science Press, Beijing, pp. 1–451.
Palynology Group of Paleobotany Research Office, Beijing Institute of Botany, Chinese Academy of Sciences, 1982. Pollen Morphology of Angiosperm in Tropical and Subtropical China. Science Press, Beijing, pp. 1–453.
Peng, J., 2012. Research on the place names culture of Weizhou island in the Beibu Gulf. J. Guangxi Normal Univ.: Philosophy and Social Sciences Edition 48 (3), 12–18 (in Chinese).
Prach, K., Walker, L.R., 2011. Four opportunities for studies of ecological succession. Trends Ecol. Evol. 26 (3), 119–123.
Qi, F., Li, G.Z., Sun, Y.F., Liang, W., Du, J., 2003. Basic geomorphologic features of the Weizhou island of the Beibu bay. Adv. Mar. Sci. 21 (1), 41–50 (in Chinese).
Ramankutty, N., Graumlich, L., Achard, F., Alves, D., Chhabra, A., DeFries, R.S., Foley, J. A., Geist, H., Houghton, R.A., Goldewijk, K.K., Lambin, E.F., 2006. Global land-cover change: recent progress, remaining challenges. Land-use and Land-Cover Change: Local Processes and Global Impacts, pp. 9–39.
Rodrigues, E., Cohen, M.C., Liu, K.B., Pessenda, L.C., Yao, Q., Ryu, J., Rossetti, D., de Souza, A., Dietz, M., 2021. The effect of global warming on the establishment of mangroves in coastal Louisiana during the Holocene. Geomorphology 381, 107648.
Rodrigues, E., Cohen, M.C.L., Pessenda, L.C.R., França, M.C., Magalhaes, E., Yao, Q., 2022. Poleward mangrove expansion in South America coincides with MCA and CWP: a diatom, pollen, and organic geochemistry study. Quat. Sci. Rev. 288, 107598.
Russell, J.C., Kueffer, C., 2019. Island biodiversity in the anthropocene. Annu. Rev. Environ. Resour. 44, 31–60.
Shu, J.W., Wang, W.M., Chen, W., 2007. Holocene vegetation and environment changes in the NW taihu plain, jiangsu province, east China. Acta Micropalaeontol. Sin. 24 (2), 210–221 (in Chinese).
Smith, R.K., Pullin, A.S., Stewart, G.B., Sutherland, W.J., 2012. Effectiveness of predator removal for enhancing bird populations. Conserv. Biol. 24 (3), 820–829.
Tang, L., Mao, L., Lü, X., Ma, Q., Zhou, Z., Yang, C., Kong, Z., Batten, D.J., 2013. Palaeoecological and palaeoenvironmental significance of some important spores and micro-algae in Quaternary deposits. Chin. Sci. Bull. 58, 3125–3139.
Trueman, M., d'Ozouville, N., 2010. Characterizing the Galapagos terrestrial climate in the face of global climate change. Galapagos Research 67, 26–37.
Tang, L., Mao, L., Shu, J., Li, C., Shen, C., Zhou, Z., 2016. An Illustrated Handbook of Quaternary Pollen and Spores in China. Science Press, Beijing, pp. 1–601 (in Chinese).
Vésteinsson, O., McGovern, T.H., Keller, C., 2002. Enduring impacts: social and environmental aspects of Viking age settlement in Iceland and Greenland. Arctic Anthropol. 39 (1), 1–28.
Vieira, I.C.G., Toledo, P.D., Silva, J.D., Higuchi, H., 2008. Deforestation and threats to the biodiversity of Amazonia. Braz. J. Biol. 68, 949–956.
Wang, F.X., Qian, N.F., Zhang, Y.L., Yang, H.Q., 1995. Pollen Morphology of Chinese Plants. Science Press, Beijing (in Chinese).
Wang, G.Z., Quan, S.Q., Lü, B.Q., 1991. Evolution of modern sedimentary environments and sedimentations in the Weizhou Island area, South China Sea. Mar. Geol. Quat. Geol. 11 (1), 69–82 (in Chinese).
Wang, M., Meng, H., Huang, L., Sun, Q., Zhang, H., Shen, C., 2020. Vegetation succession and forest fires over the past 13000 years in the catchment of Yangzonghai Lake, Yunnan. Quat. Sci. 40 (1), 175–189 (in Chinese).
Wang, W., Li, C., Shu, J., Chen, W., 2019. Changes of vegetation in southern China. Sci. China Earth Sci. 62, 1316–1328.
Wang, Z., Cao, H., Xiao, Y., He, J., Zhang, S., Dong, G., 2021. Prehistoric human activity and changes in living environment at Shalongka site, northeast Tibetan Plateau. Quat. Sci. 41 (1), 201–213 (in Chinese).
Waycott, M., Duarte, C.M., Carruthers, T.J., Orth, R.J., Dennison, W.C., Olyarnik, S., Calladine, A., Fourqurean, J.W., Heck Jr, K.L., Hughes, A.R., Kendrick, G.A., 2009. Accelerating loss of seagrasses across the globe threatens coastal ecosystems. Proc. Natl. Acad. Sci. USA 106 (30), 12377–12381.
Wentworth, C.K., 1922. A scale of grade and class terms for clastic sediments. J. Geol. 30 (5), 377–392.
Willis, K.J., MacDonald, G.M., 2011. Long-term ecological records and their relevance to climate change predictions for a warmer world. Annu. Rev. Ecol. Evol. Syst. 42, 267–287.
Wilmshurst, J.M., Moar, N.T., Wood, J.R., Bellingham, P.J., Findlater, A.M., Robinson, J. J., Stone, C., 2014. Use of pollen and ancient DNA as conservation baselines for offshore islands in New Zealand. Conserv. Biol. 28 (1), 202–212.
Yao, Q., Liu, K.B., 2017. Dynamics of marsh-mangrove ecotone since the mid-Holocene: a palynological study of mangrove encroachment and sea level rise in the Shark River Estuary, Florida. PLoS One 12 (3), e0173670.
Yao, Q., Liu, K.B., Aragón-Moreno, A.A., Rodrigues, E., Xu, Y.J., Lam, N.S., 2020b. A 5200-year paleoecological and geochemical record of coastal environmental changes and shoreline fluctuations in southwestern Louisiana: implications for coastal sustainability. Geomorphology 365, 107284.
Yao, Q., Liu, K.B., Cohen, M.C.L., Fan, D.D., Rodrigues, E., Maiti, K., de Souza, A.V., Aragón-Moreno, A.A., Rohli, R., Yin, D.X., Pessenda, L.C.R., 2022a. Mangrove expansion at poleward range limits in North and South America: late-Holocene climate variability or Anthropocene global warming? Catena 216, 106413.
Yao, Q., Liu, K.B., Rodrigues, E., 2022b. Pre–treatment method to avoid contamination for radiocarbon dating of organic–rich coastal deposits. MethodsX 9, 101745.
Yao, Q., Liu, K.B., Rodrigues, E., 2023c. An improved preparation procedure for pollen samples from coastal clastic sediments. MethodsX 10, 102016.
Yao, Q., Liu, K.B., Rodrigues, E., Bianchette, T., Aragón-Moreno, A.A., Zhang, Z., 2020a. A geochemical record of Late-Holocene hurricane events from the Florida Everglades. Water Resour. Res. 56 (8), e2019WR026857.
Yao, Q., Liu, K.B., Rodrigues, E., Fan, D., Cohen, M., 2023b. A palynological record of mangrove biogeography, coastal geomorphological change, and prehistoric human activities from Cedar Keys, Florida, USA. Sci. Total Environ. 859, 160189.
Yao, Q., Liu, K.B., Zhang, Z., Rodrigues, E., Cohen, M., Maiti, K., Yang, Y., 2023d. What are the most effective proxies in identifying storm-surge deposits in paleotempestology? A quantitative evaluation from the sand-limited, peat-dominated environment of the Florida coastal everglades. G-cubed 24 (3), e2022GC010708.
Yao, Q., Liu, K.B., Fan, D.D., Cohen, M.C.L., De Oliveira, P.E., Rodrigues, E., 2023a. Eco-morphological Evolution of the Bolivar Peninsula (Texas, U.S.A.) during the Last 2,000 Years: A Multi-proxy Record of Coastal Environmental Changes. Quat. Sci. Rev. 308, 108064.
Yu, J.J., Peng, B., Lan, Y., Wu, B., Wang, J.L., Ding, D.L., Lao, J.X., Li, S.L., Dai, L., 2021. Palynological record revealed anthropogenic deforestation, sea level and climate changes since marine isotope stage 5a in the northeastern coast of Fujian Province. Earth Science 46, 281–292 (in Chinese).
Yue, Y., He, L., Zheng, Z., Chen, C., Wan, Q., Tang, Y., Huang, K., 2024a. Late Holocene vegetation succession, climate change, and fire history in western Guizhou. Quat. Sci. 44 (1), 112–127. https://doi.org/10.11928/j.issn.1001-7410.2024.01.09 (in Chinese).
Yue, Y., Tang, L., Yu, K., Huang, R., 2024b. Coral records of Mid-Holocene sea-level highstands and climate responses in the northern South China Sea. Acta Oceanol. Sin. 43, 43–57.
Yue, Y., Tang, L., 2023. Characteristics of sea level changes in the northern South China Sea since the Holocene and prediction of the future trends. Marine Geology Frontiers 39 (2), 1–16. https://doi.org/10.16028/j.1009-2722.2022.193 (in Chinese).
Yue, Y., Yu, K., Tao, S., Zhang, H., Liu, G., Wang, N., Jiang, W., Fan, T., Lin, W., Wang, Y., 2019. 3500-year western Pacific storm record warns of additional storm activity in a warming warm pool. Palaeogeogr. Palaeoclimatol. Palaeoecol. 521, 57–71.
Yue, Y., Zheng, Z., Rolett, B.V., Ma, T., Chen, C., Huang, K., Lin, G., Zhu, G., Cheddadi, R., 2015. Holocene vegetation, environment and anthropogenic influence in the Fuzhou Basin, southeast China. J. Asian Earth Sci. 99, 85–94.

Zhang, R., Zhang, R., Yu, K., Wang, Y., Huang, X., Pei, J., Wei, C., Pan, Z., Qin, Z., Zhang, G., 2018. Occurrence, sources and transport of antibiotics in the surface water of coral reef regions in the South China Sea: Potential risk to coral growth. Environ. Pollut. 232, 450–457.

Zhang, Y., Yu, K., Fan, T., Yue, Y., Wang, R., Jiang, W., Xu, S., Wang, Y., 2020. Geochemistry and petrogenesis of Quaternary basalts from Weizhou Island, northwestern South China Sea: Evidence for the Hainan plume. Lithos 362, 105493.

Zhang, Z., Yao, Q., Liu, K.B., Li, L., Yin, R., Wang, G., Sun, J., 2021a. Historical flooding regime along the Amur River and its links to East Asia summer monsoon circulation. Geomorphology 388, 107782.

Zhang, Z., Yao, Q., Xu, Q., Jiang, M., Zhu, T., 2021b. Hydrological and palynological evidence of wetland evolution on the Sanjiang Plain (NE China) in response to the Holocene East Asia summer monsoon. Catena 203, 105332.

Zheng, J., Liu, Y., Hao, Z., Ge, Q., 2021. State-of-art and perspective on global synthesis studies of climate change for the past 2000 years. Quat. Sci. 41 (2), 309–322 (in Chinese).

Zhong, C.L., Bai, J.Y., Zhang, Y., 2005. Introduction and conservation of *Casuarina* trees in China. For. Res. 18 (3), 345–350 (in Chinese).

Zhu, X.D., Li, H.W., Shi, F., 2012. Records of Weizhou Island. Guangxi People's Publishing House, Nanning, pp. 1–359 (in Chinese).

Zimmerman, N., Hughes, R.F., Cordell, S., Hart, P., Chang, H.K., Perez, D., et al., 2007. Patterns of primary succession of native and introduced plants in lowland wet forests in eastern Hawai'i. Biotropica 39 (4), 355–366.